ChemPlusChem

A Multidisciplinary Journal Centering on Chemistry

Accepted Article

Title: Valeric Biofuels from Biomass-Derived γ-Valerolactone: A Critical Overview of Production Processes

Authors: Karla Geraldine Martínez Figueredo, Francisco A. Martínez, Darío Jobino Segobia, and Nicolás Maximiliano Bertero

This manuscript has been accepted after peer review and appears as an Accepted Article online prior to editing, proofing, and formal publication of the final Version of Record (VoR). The VoR will be published online in Early View as soon as possible and may be different to this Accepted Article as a result of editing. Readers should obtain the VoR from the journal website shown below when it is published to ensure accuracy of information. The authors are responsible for the content of this Accepted Article.

To be cited as: *ChemPlusChem* **2023**, e202300381

Link to VoR: https://doi.org/10.1002/cplu.202300381

WILEY VCH

REVIEW

Valeric Biofuels from Biomass-Derived γ-Valerolactone: A Critical Overview of Production Processes

Karla G. Martínez Figueredo, Francisco A. Martínez, Darío J. Segobia, Nicolás M. Bertero *[a]
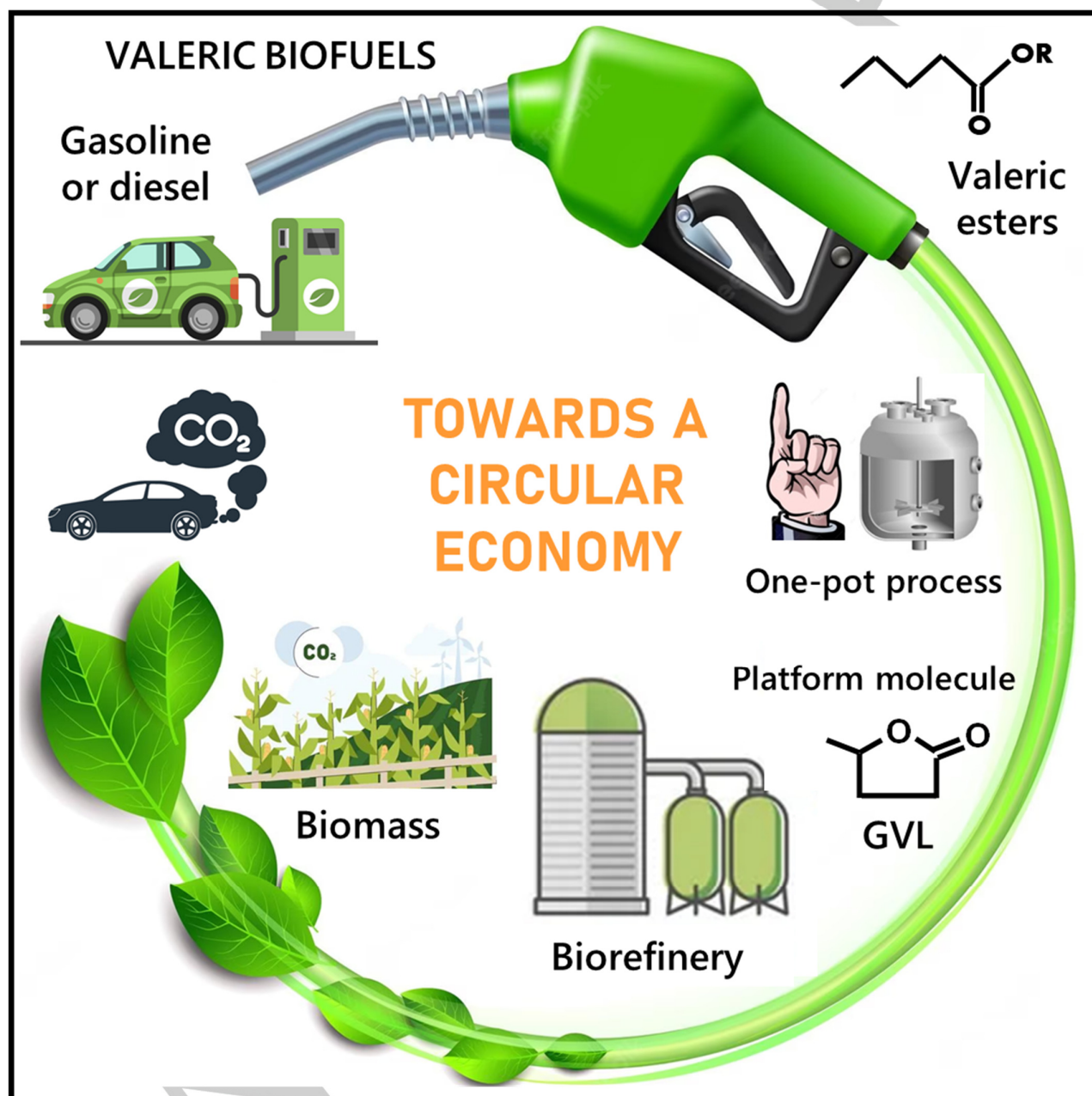
[a]   Ph.D. K.G. Martínez Figueredo; BEng. F.A. Martínez; Ph.D. D.J. Segobia; Ph.D. N.M. Bertero
       Catalysis Science and Engineering Research Group (GICIC)
       Instituto de Investigaciones en Catálisis y Petroquímica (INCAPE), UNL-CONICET, Centro Científico Tecnológico.
       Paraje El Pozo, Santa Fe (3000), Santa Fe, Argentina.
       E-mail: nbertero@fiq.unl.edu.ar

Abstract: This review analyzes critically the production of valeric biofuels from γ-valerolactone, a relevant biomass-derived platform molecule. Initially, the main properties of valeric esters as fuels for spark- and compression-ignition engines are summarized. Then, catalytic routes to valeric esters from γ-valerolactone are meticulously analyzed, describing the acid- and metal-catalyzed reactions taking part in the tandem catalysis. Only works focused on the production of the valeric biofuels were considered, excluding the cases where these esters were observed in minor amounts or as byproducts. The role of the appropriate selection of the support, catalytic species, catalyst preparation and experimental conditions on the valeric ester productivity are thoroughly commented. Finally, some concluding remarks and perspectives are given, mentioning the areas where additional efforts must be done in order to turn the dream of a massive and renewable valeric biofuel production into a reality.

1. Introduction

Mankind supplies regarding energy and chemicals rely heavily on fossil resources such as petroleum and gas. Although it is difficult to predict the exact date of the depletion of these fossil resources [1], there is an urgent need for promoting the energy transition at the light of the accumulation of CO_2 in the atmosphere, a greenhouse gas that causes global warming. Unfortunately, research efforts in the direction of the development of a new and more sustainable energy matrix were somehow postponed in the last decade, when large reserves of shale oil and gas were discovered worldwide [2][3]. These additional fossil resources though change the basis of the petrochemical industry during several years undoubtedly have not brought a solution for the sustainability of the energy matrix that still depends strongly on non-renewable fossil resources.

A significant portion of the energy demand in developed countries is ascribed to the transportation sector. For instance, in EEUU, during 2020 the energy consumed for transportation purposes accounted for about 26.1% of the total energy consumed, but during 2018 and 2019, previous to the traffic restrictions for COVID-19 pandemic, represented the 28% [4]. To make matters worse, 92% of this energy demanded for transportation is supplied with fossil-fuels and this is causing a significant increase in the concentration of atmospheric CO_2.

For all the previous reasons, the scientific research has been working incessantly for developing second generation biofuels, i.e. alternative fuels derived from non-edible raw materials [5][6]. In this sense, the most promising raw material for the production of biofuels is the lignocellulosic biomass due to: (a) it is obtained from agricultural waste or non-food crops; (b) it is an relatively inexpensive and abundant raw material (only in EEUU 1.3 billion of dry biomass per year can be produced [7]); 3) it can provide the energy of 30-160 billion barrels of oil equivalent (bboe) per year worldwide [8]. Nevertheless, to transform the lignocellulose biomass consisting mainly of cellulose, hemicellulose and lignin (highly oxygenated natural polymers) [9], into biofuels is a relatively complex chemical task. The first approaches for achieving this task were based on the biomass conversion by thermochemical processes, e.g., gasification, pyrolysis and liquefaction, very well-treated in previous reviews [6][10]. Nevertheless, the main disadvantages shown by these routes are: (i) fuels containing innumerable compounds; (ii) relatively low fuel energy density due to the high oxygenated content; (iii) high acidity and (iv) storage-related issues [6].

With the aim of connecting the processing technology of the biomass with the one of the petroleum already developed, the concept of biomass-derived platform molecules arose [11]. This made possible to draw the well-known strategy comprising: (a) deconstruction of lignocellulose into platform molecules such as levulinic acid (LA) [12] and γ-valerolactone (GVL) [13][14]; (b) conversion of these platform chemicals into biofuels [10,15–17]. Even more, the hydrogenation of LA into GVL has been widely reported by several authors [18] and reviewed by Wright and Palkovits, confirming that GVL has also become a relevant platform molecule [19].

The conversion of LA and GVL into biofuels and fuel additives comprises several catalytic chemical transformations that, in many cases, are carried out in a one-pot process. The combination of multiple catalytic reactions in single pot operations carried out by multifunctional catalysts improves the process integration, avoiding isolation and purification of intermediates and reducing the formation of unwanted by-products [20]. Due to the relevance and the increasing number of works regarding catalytic conversion of LA and GVL into biofuels and fuel additives, several authors have contributed with reviews and critical reviews in this field of research [6,10,15,16,21–23].

Among different second-generation biofuels produced from LA or GVL, valeric esters (VE) are of especial interest. These pentanoic acid (PA) esters show a better fuel performance than current alternative biofuels such as ethanol, n-butanol, GVL, ethyl levulinate and 2-methyltetrahydrofuran due to more appropriate combustion, polarity, volatility, and ignition properties. Furthermore, as it is explained in section 2, an important feature of VE is the fact that they share the same hydrocarbon backbone of PA, but modifying the alkyl chain length in the carboxylic group (-OR) leads to different kind of biofuels, from gasoline- to diesel-compatible, providing a flexible range of fuel properties.

Previously cited reviews about catalytic conversion of LA and GVL into biofuels and fuel additives covered the production of VE only partially, because when they were published only very few relevant scientific contributions about valeric biofuels were available. It is worth mentioning that since 2014, though not many works were published, important advances in this field were reported and an updated mini-review about this matter would be a valuable contribution to this field of research. In this sense, most of these works employed GVL as reactant, though there are some reports of the integration of hydrogenation of LA into GVL and the conversion to VE. In all the cases, the production of these esters involves tandem catalysis in one-pot processes and its development and industrial implementation are still in an early stage, even today, 12 years after the synthesis of these relevant compounds was firstly reported by Lange et al. [24]. It is worth noticing that the production of these esters from platform molecules such as GVL and LA has been mainly studied in batch mode at the light that there are some issues to be solved before moving to continuous processes [16].

REVIEW

In the following sections the properties that make valeric esters attractive biofuels are summarized and the reported one-pot processes for the production of these esters from GVL or LA are thoroughly analyzed. Particular contributions focused on the combination of experimental methods and theoretical calculations for understanding the reaction mechanism taking place during the ring-opening of GVL towards the formation of VE or intermediates are described, as well. However, scientific contributions not focused on VE production or where VE were formed only as byproducts were not considered for this review. Finally, we provide some future perspectives about this field of research.

2. Valeric esters as cellulosic transportation fuels

The effectiveness of fuels in internal combustion engines depends on their physicochemical properties because these properties influence the engine ignition delay time, engine-out emissions, rate and period of combustion, engine pressure and temperature [25]. For instance, a relatively high BRON increases knock resistance, engine efficiency, and curtails engine-out emissions. The lower heating value (LHV) determines the energy content of the fuel, whereas a relative high oxygen content can reduce soot and particulate matter emissions.

As mentioned previously, the catalytic production and use as biofuels of VE, or pentanoic acid esters, were firstly reported by Lange et al. in 2010 [24]. In that pioneering work, these researchers not only explained the consecutive chemical reactions needed to obtain valeric esters from biomass-derived platform molecules, but also assessed their compatibility with traditional fossil fuels in order to analyze whether vehicle modifications and/or the distribution network were necessary. Here, only a summary of the main fuel properties of VE is presented and we refer the reader to the original references for details concerning these properties [24,26–28]. Depending on the alkyl chain length, VE show different polarity, volatility, and ignition properties that make them suitable for biofuels compatible with gasoline or diesel. As shown in Table 1, the physicochemical properties of valeric esters [27] are comparable and/or, in some cases, even better than those of petroleum-based fuels [25], first-generation and other second-generation biofuels [29]. Therefore, VE have good potential as alternative fuels to be used in internal combustion engines.

Initially, the basic properties that Lange et al. analyzed were polarity (Hildebrand solubility parameter), volumetric energy content, normal boiling point and octane number or cetane number, i.e. useful properties for describing ignition features of
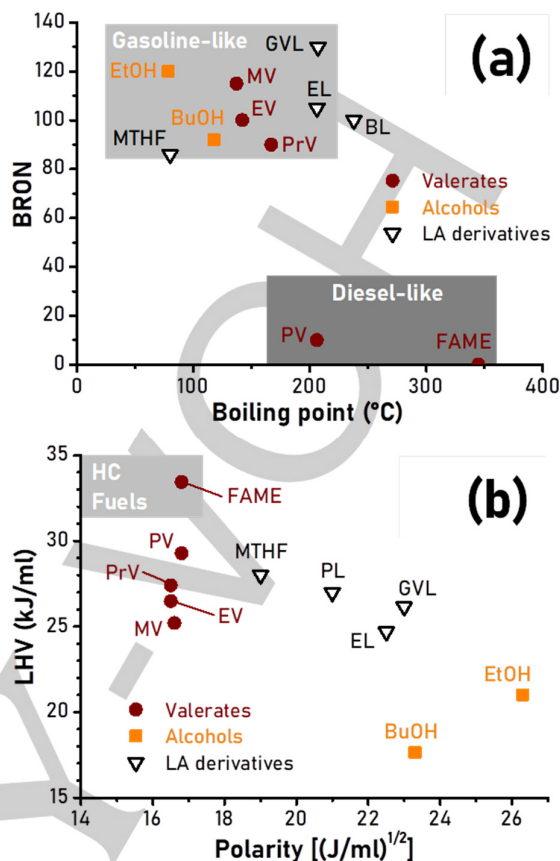

Figure 1: Relevant parameters in the evaluation of fuel performance: (a) blending research octane number (BRON) vs. boiling point and (b) lower heating value (LHV) vs. polarity using Hildebrand´s solubility parameter [MV, EV, PrV and PV are methyl, ethyl, propyl and pentyl valerate, respectively]. Grey areas represent property windows of hydrocarbon fuels (HC). Adapted from Ref. [24] Copyright (2010), with permission from Wiley-VCH.

gasoline and diesel, respectively. These authors compared the values of these properties for methyl (MV), ethyl (EV), propyl (PrV) and pentyl valerate (PV) with other biofuels such as fatty acid methyl esters (FAME) and other chemicals that also exhibit fuel properties as alcohols (EtOH, BuOH), GVL, ethyl levulinate (EL), butyl levulinate (BL), methyltetrahydrofuran (MTHF), etc. and the results of this first evaluation are shown in Figure 1. Valerate esters exhibit acceptable energy content, similar to some alcohols and GVL, but slightly lower than FAME. Besides, VE show a similar polarity than FAME but lower than the values

Table 1: Physicochemical properties of the main fossil fuels, first-generation (bioethanol and biodiesel) and second-generation biofuels (green diesel and valeric esters). [gasoline-type fuels: petroleum gasoline, bioethanol, ethyl and propyl valerate; diesel-type fuel: petroleum ULSD, biodiesel, green diesel, butyl and pentyl valerate].

| Property	Petroleum gasoline	Bioethanol	Ethyl valerate	Propyl valerate	Petroleum ULSD	Biodiesel (FAME)	Green Diesel	Butyl valerate	Pentyl valerate
Oxygen (wt%)	0	35	24.6	22.2	0	11	0	20.2	18.6
Density (kg/l)	0.72-0.75	0.79	0.874	0.870	0.84	0.88	0.78	0.868	0.874
Sulphur (ppm)	< 30	< 1	< 1	< 1	< 10	< 1	< 1	< 1	< 1
Low heating value (MJ/kg)	42.13	26.9	30.3	31.5	43	38	44	32.6	33.5
Distillation range (℃)	25-220	78.3	142	167	200-350	340-355	265-320	187	206
BRON	96	108.6	100	90	n.a.	n.a.	n.a.	n.a.	10
Cetane	10-15	8	17.1	n.a.	40	50-65	70-90	24.5	30.3
Stability	Good	Good	Good	Good	Good	Marginal	Good	Good	Good

ULSD: is ultra low sulphur diesel.
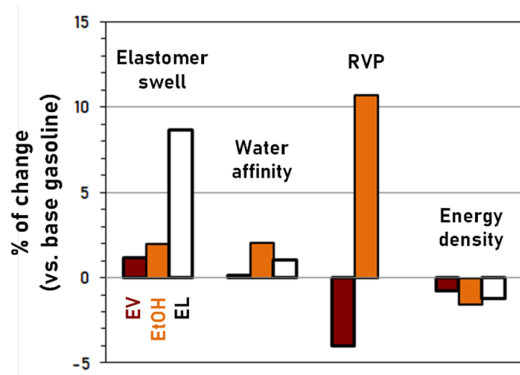
Figure 2: Relative changes in fuel properties when ethyl valerate (EV, ■), ethanol (EtOH, ■) and ethyl levulinate (EL, □) are blended at 5% in gasoline (the water affinity is measured for neat biofuel). RVP: Reid vapor pressure.

of some alternative biofuels such as alcohols, GVL, MTHF and levulinates.

Regarding the compatibility with fossil fuels, EV can be blended up to 20 vol% with regular gasoline meeting the research (RON) and motor octane number (MON) specification for European gasoline. In the case of PV, other authors have demonstrated that it can be blended with diesel also up to 20 vol% without causing a significant impact on the fuel properties or engine efficiency and emissions [26].

Secondly, Lange et al. compared the relative changes in other fuel properties such as elastomer swell, water affinity, reid vapor pressure (RVP) and energy density when base gasoline was blended with 5% of EV, ethanol and ethyl levulinate. As Figure 2 shows, the addition of 5% of EV only increases 1.5% the elastomer swell and reduces 4% the water pickup of the gasoline, thanks to the relatively low polarity of this ether in comparison with EtOH and ethyl levulinate. Besides EV has a higher energy density than EtOH, lowering only 0.5% the energy density of the mixture in contrast with 1.5% with EtOH. Furthermore, EV with a higher boiling point that EtOH makes unnecessary the removal of light hydrocarbons from the gasoline before blending with the biofuel.

In the case of bulkier alkyl chain, butyl and pentyl valerates are suitable for diesel pools. In particular pentyl valerate (PV) exhibits a better volatility and cold-flow properties than FAME for diesel, though the energy density is some lower (Figure 2). Besides, Lange et al. proposed the production of di- and trivalerates, esterifying pentanoic acid with ethylene and propylene glycols. Although these heavier esters are also compatible with diesel pools regarding their solubility and volatility, they show a low cetane number that limits their proportion at regulated valued. All these heavier valerate esters improve the lubricity properties of the diesel mixture.

Finally, Lange et al. not only developed catalytic processes for producing valeric biofuels and measured their fuel properties, but also tested a blend of 15 vol% EV in regular gasoline during an accumulative 250,000 km road trial, using ten vehicles (including new and used cars). The researchers followed the evolution of performance, engine status, exhaust emissions, etc., concluding that the addition of 15 vol% EV in the regular gasoline does not impact significantly on engine wear, oil degradation, vehicle durability, engine deposits or regulated tailpipe emissions. In addition, the good octane number of EV improved the engine power, though a small loss in volumetric fuel economy was measured compared to non- oxygenated

gasoline by the lower energy density. Last, but not the least, this blend containing 15 vol% EV showed good stability after four months, without consequences on fuel storage and related equipment such as tanks, pipes, pumps and filters.

On the other hand, an important physical property that impacts on transportation costs is the density of the fuel. Typical gasoline and diesel show density values of 720 kg/m^3 and 850 kg/m^3, respectively. In the case of the compatible valeric biofuels, values of about 874 kg/m^3 were determined for ethyl and pentyl valerates [27], i.e. values 21% and 3% higher than the traditional fossil fuels. This means that costs for transportation of the valeric biofuels, especially in the case of ethyl valerate, will be higher than for the traditional gasoline and this could have a significant impact in the economics of the biofuel implementation as the margins in the transportation fuel market are rather small and biorefineries are often far from large demand centers [30].

3. Catalytic routes to valeric biofuels from biomass-derived platform molecules

Lignocellulosic biomass can be converted into valeric biofuels in biorefineries by using multiple catalytic transformations [31]. The first of them starting from the lignocellulosic raw materials are hydrolysis reactions, which convert the biomass into simpler platform molecules such as levulinic acid (LA) [32]. Then, the conversion of LA into GVL by hydrogenation has been reported by many authors and satisfactorily reviewed by Wright and Palkovits [19]. Finally, both platform molecules LA or GVL can be converted into valeric biofuels or fuel additives through specific catalytic transformations involving multifunctional catalysis [16].

3.1. Valeric esters production from LA

Lange et al. proposed a novel route for producing valeric esters from lignocellulosic raw materials based on the following consecutive chemical steps: (1) acid hydrolysis of lignocellulosic materials to obtain levulinic acid (LA); (2) hydrogenation of LA into GVL; (3) hydrogenation of GVL into valeric or pentanoic acid (PA) and (4) esterification of PA with alcohols or glycols to produce the valeric esters [24]. Initially, these authors explored under continuous reaction conditions the LA hydrogenation into GVL at 200 °C, 40 bar of H$_2$, H$_2$/LA molar ratio of 5:1 and using a WHSV equal to 9 h^{-1} over 50 catalysts, among them monometallic and bimetallic Pt-based catalysts supported on C, SiO$_2$, ZrO$_2$ and TiO$_2$. Over Pt(1%)/TiO$_2$ a LA conversion of about 95% and a GVL selectivity of 95%, with relatively high GVL productivity (10 g$_{GVL}$.g$_C^{-1}$.h^{-1}) was attained with marginal deactivation after 100 h. The consecutive conversion of GVL to PA was also investigated over 150 catalysts, obtaining the best result over a Pt/HZSM-5/SiO$_2$, with a PA selectivity of 80-85% at 250 °C, 10 bar of H$_2$ and a H$_2$/GVL molar ratio of 9:1 using a WHSV equal to 2 h^{-1}. However, due to a strong deactivation, for maintaining this performance over 1500 h, intermittent regeneration by H$_2$ strips at 400 °C was necessary. In this sense, Pt/SiO$_2$-Al$_2$O$_3$ samples though initially were less active, deactivated much slower and remained active after 200-300 h of run. Finally, for the esterification of PA to VE, an acid ion exchange resin was employed, reaching a VE selectivity higher than 95%. However, these authors not only studied the isolated catalytic steps, but also explored the conversion of (1) LA into PA; (2) LA into EV and (3) GVL into PV, evaluating options for process integration. In the first case, Pt/ZSM-5 was reported as

the best catalyst, operating the reactor with a temperature gradient or performing the conversion under reactive distillation conditions. In the second case, the authors reported the production of EV by simultaneously feeding LA and ethanol (EtOH) in a reactive distillation reactor containing a bifunctional catalyst (Pt/ZSM-5 or Pt/TiO$_2$ + H$_2$SO$_4$) in the lower segment and another of hydrogenation (Pt/TiO$_2$) in the rectification segment. Thus, LA was hydrogenated to GVL over the hydrogenation catalyst, then GVL reacted with ethanol (EtOH) to become ethyl pentenoate (EP) in the presence of the acid catalyst, and finally EP was hydrogenated to EV over Pt/TiO$_2$. In this way, they minimized the production of undesirable ethyl ether or dipentyl ether, a compound that they obtained together with PA and EV through another process, in which they fed EtOH or PL and LA as a physical or chemical mixture (in the form of ethyl or pentyl levulinate) on a zeolite-based catalyst. In the last case, the conversion of GVL into PV was performed at 275 °C, 10 bar of H$_2$, a H$_2$/GVL molar ratio of 9:1 and using a WHSV equal to 2 h^{-1}, obtaining a PV and PA yield of 15 and 31%, respectively over Pd(0.3%)/TiO$_2$. Therefore, these authors not only introduced for the first time the valeric esters into the field of 2nd generation biofuels, but also highlighted the key role of PA in this catalytic pathway for the complete manufacturing process of valeric biofuels.

Additionally, Lange and Haan patented the process [33], where the synthesis of PV is carried out by the conversion of GVL in the presence of hydrogen and a heterogeneous catalyst free of zeolite, composed of a hydrogenating metal supported on a metal oxide or a mixed oxide, preferably on a metal dioxide such as TiO$_2$ or ZrO$_2$ and free of any heterogeneous or homogeneous strong acid catalyst, such as heteropolyacids or mineral acids (H$_2$SO$_4$ or H$_3$PO$_4$). The hydrogenation metal of the catalyst involves a metal from any of groups 7 to 11 of the periodic table of the elements, such as Ni, Rh, Pd, Pt, Re, Ru, Ir or a combination of two or more; most suitable being Pt, Pd or a

combination of them. Regarding the metal load, they reported values preferably between 0.1 to 2%wt. The process is carried out at temperature between 250-350 °C and at any pressure, as long as it is low enough to prevent condensation of the feed component. Additionally, they detailed that the catalytic experiments were carried out in gas phase using supported Pt and Pd catalysts prepared by incipient wetness impregnation using metal salts of H$_2$PtCl$_6$·6H$_2$O and Pd(NH$_3$)$_4$(NO$_3$)$_2$, respectively. Next, the impregnated solids were calcined in air flow at 400 and 600 °C for 3 h. Then, the GVL conversion process was carried out by loading 0.5 g of catalyst in the reactor and reducing it at 400 °C in H$_2$ flow for 1 h, subsequently, the system was cooled to the reaction temperature before feeding GVL reactant. The authors observed a higher conversion of GVL when the Pt/TiO$_2$ and Pd/TiO$_2$ catalysts were calcined at 400 °C instead of 600 °C. They also observed that the PV/PA ratio was higher when Pt-based catalysts were used instead of Pd. Finally, it was determined that increasing both the metal loading the reaction temperature favors the GVL conversion, though no significant changes in the formation of PV were detected. It is worth highlighting that these authors studied the GVL conversion to PV in a continuous process.

Following the approach of Lange et al., the one-pot conversion of LA to PA and/or VE was reported by several authors employing different combinations of metal function and acidic support. For an exhaustive revision of these works up to 2019, the work of Yu et al. is strongly recommended [34]. Three years later, in 2022 another interesting review about this matter was published by Pothu et al., but focusing the attention mainly on the production of PA from different biomass-derived platform molecules [35].

Although LA was the first biomass-derived platform molecule for the production of second-generation biofuels [7], due to GVL can be easily obtained from LA and GVL is a relatively stable intermediate, this lactone has become also a relevant platform
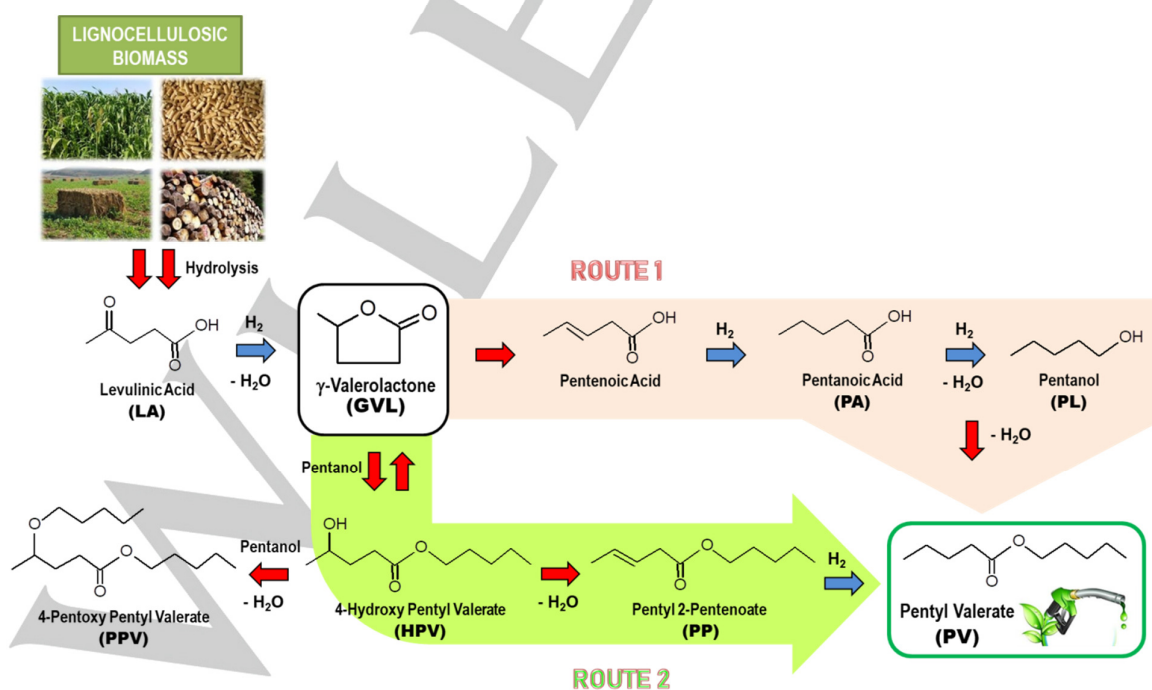

Figure 3: Reported reaction schemes for the production of pentyl valerate (PV) from biomass-derived γ-valerolactone (GVL) involving multiple catalytic transformations (➡ acid-catalyzed reactions, ➡ metal-catalyzed reactions).

molecule [15]. Even more, the use of GVL as raw material for producing valeric esters avoids some side reactions such as the LA etherification in the isolated –OH group and/or esterification in the presence of acid catalysts. Thus, the recognition of GVL as a relevant biomass-derived platform molecule, the different reaction pathways towards VE from GVL (involving or not the use of an alcohol also as reactant not very well described in the published reviews about VE production from LA) and the increasing number of works employing GVL as reactant for obtaining valeric biofuels were the main reasons that motivated the writing of this work.

3.2. Valeric esters production from GVL

At the light of the wide spectrum of processes, catalysts and reaction conditions for converting LA into GVL [19], and the properties of GVL that show it is both stable (can be stored without decomposition or degradation with time even in the presence of oxygen or water) and reactive enough to produce a variety of chemicals, this cyclic ester with four carbon atoms and one oxygen atom has gained increasing relevance as biomass-derived platform molecule [15]. Regarding its use in the fuel field, it is more attractive to use as raw material to obtain more energy dense biofuels such as VE than its direct use as fuel.

In 2013 Alonso et al. reviewed the reaction pathways for the conversion of GVL into different fuels such as MTHF (gasoline blender), aromatics (fuel additive), C_{8+} alkanes (jet fuel), C_9 alkanes (diesel/gasoline), C_{18-27} alkanes (diesel) and valeric esters (biodiesel) [15]. However, at that time only two works had been published about the VE production from GVL [24][36]. Since 2013 several researchers have focused their attention on the valeric biofuel production from GVL, employing a wide variety of catalytic systems and reaction conditions. Depending on the reaction conditions, mainly on the presence of an alcohol as reactant, the conversion of GVL into VE can take place through two different mechanisms. As an example, the production of pentyl valerate (PV) biofuel from biomass-derived GVL is shown in Figure 3, where both routes are depicted.

Lange et al. proposed their ROUTE 1 for producing valeric esters from lignocellulosic raw materials based on the consecutive chemical steps previously described in section 3.1 [24]. In this route, PA is a key intermediate, detectable in important amounts in the reaction mixture. However, this route, though it was the first reported, it is not the only one for the production of VE starting from GVL. An alternative reaction path was introduced by Chan-Thaw et al. in 2013 (Figure 3), carrying out the GVL conversion in the presence of an alcohol containing the hydrocarbon chain of the intended valeric ester [36]. When the conversion of GVL takes place using this alcohol also as reactant (ROUTE 2) the reaction path to VE is completely different from ROUTE 1 and PA is not observed as intermediate. In the case of using pentanol (PL) as reactant, the one-pot catalytic process involves the following transformations (ROUTE 2 in Figure 3): (a) the acid-catalyzed ring-opening of GVL by nucleophilic addition of PL to the carboxylic group to form 4-hydroxy pentyl valerate (HPV); (b) acid-catalyzed intramolecular dehydration of HPV into pentyl 2-pentenoate (PP) and (c) metal-catalyzed hydrogenation of C=C double bond of PP to produce pentyl valerate (PV). However, depending on the characteristics of the acid catalyst and reaction conditions, the HPV intermediate can also react with another PL molecule to form 4-pentoxy pentyl valerate (PPV), an undesirable product. Besides, another possible side reaction over bifunctional catalysts is the

conversion of GVL into undesirable 2-methyltetrahydrofurane (MTHF) by hydrogenation and hydrogenolysis (not shown in Figure 3).

Both reaction routes to VE (ROUTE 1 and 2) depend on the use of multifunctional catalysts, in particular metal/acid bifunctional catalysts, to perform efficiently the required orthogonal tandem catalysis. Beyond these pioneering works, several authors have reported other catalysts and reaction conditions. In general, it can be seen that ROUTE 1 was exclusively based on the use of a bifunctional catalyst employing an acidic support, whereas in ROUTE 2 two different approaches were used: (1) employing acid solids as supports and depositing the metal phase onto the support and (2) depositing the metal phase onto a non-acidic support (such as SiO_2), generating metal particles with a catalytically relevant Lewis acidity.

In the following subsections 3.2.1 and 3.2.2, a detailed analysis of both routes for producing valeric biofuels from the GVL platform molecule is carried out. Works dealing with the integration of LA conversion to GVL and production of VE are not considered because they have already been reviewed previously in 2019 by other authors [34]. However, several works since then have been published regarding the EV production from GVL, especially following ROUTE 2, where the EV productivity has been significantly improved in batch processes.

3.2.1. Valeric biofuel production from GVL along ROUTE 1

In this section a detailed description of the reported processes for obtaining VE along ROUTE 1 is performed, classifying the works according to the nature of the metal employed in the bifunctional catalytic system.

Before analyzing the particular contributions to this section, it is worth mentioning that the selective conversion of GVL to biofuels, or intermediates to biofuels, along ROUTE 1 depends strongly on the different C–O bond scission modes for the ring-opening of the GVL molecule. In this sense, it is relevant to point that there are three possible C-O bonds where the ring-opening can take place in the GVL molecule. As Figure 4 depicts, the ring-opening of GVL after interaction with the catalyst surface produces different products depending on the particular C-O bond cleavage. For the production of valeric esters, through the PA intermediate, the C4-O1 bond scission is the focus of the
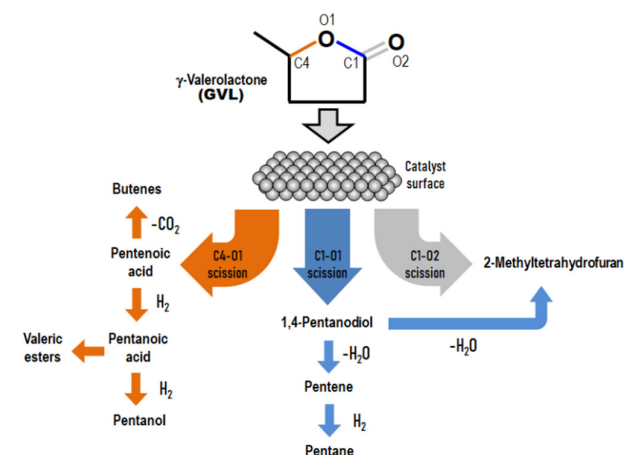
Figure 4: GVL upgrading to various fuels or fuel additives depending on the particular C-O bond cleavage and ring-opening mode of GVL over bifunctional catalysts.

attention [37][38][39]. However, both the C1-O1 and C1-O2 bond scissions can also lead to other fuels such as pentanes [40][41] or fuel additives such as 2-methyltetrahydrofuran or its precursor 1,4-pentanediol [42][43]. At the light of this, several works are combining theoretical calculations with experimental tasks in order to design an efficient bifunctional catalyst for the specific desired product. In this case, we will focus the discussion in this section not only on the experimental works performed for obtaining VE, but also on theoretical calculations that, increasingly, support the experimental results. Thus, a successful bifunctional catalyst design is achieved combining two different scientific paths that work in collaboration. However, the discussion of the following section starts with the bifunctional catalysts based on noble metals, where almost the whole work was performed experimentally and not theoretically.

3.2.1.1. Use of catalytic systems based on noble metals

After the work of Lange et al., other research groups have shown interest in the synthesis of valeric esters following ROUTE 1 (Figure 3). Yan et al. proposed other catalytic species, also based on a noble metal, to efficiently obtain PV in liquid phase starting from GVL in a batch one-pot process [44]. The catalysts, all prepared by wet impregnation, were: Pd(5%)/MCM-41, Pd(7%)/MCM-41, Pd(5%)/ZrMCM-41, Pd(3%)/HY and Pd(5%)/HY. Among these samples, it was found that the Pd/HY catalyst was the most selective towards the formation of PV and pentane, a mixture that can be also considered a biofuel. With Pd(5%)/HY and Pd(3%)/HY catalysts, no significant difference was observed in terms of activity when the metal load was varied. The reaction conditions were 0.10 g of catalyst, 5 mL of octane as solvent, 1000 rpm of stirring, a GVL/catalyst ratio of 22 (by weight), reaction temperature between 200 and 280 °C, the H_2 pressure between 40 and 80 bar and the reaction time between 12 and 36 h. From the investigation of influence of the reaction parameters on the catalytic performance it was found that the reaction time and the H_2 pressure have a crucial influence on the PV yield, since the highest PV yield (60.6%) and GVL conversion (99%) were reached at 80 bar and 30 h working at 260 °C. However, by extending the reaction time to 36 h, traces of undesirable by-products such as 1,4-pentanediol or MTHF were detected. Regarding the deactivation of the catalyst, Yan et al. carried out reuse experiments, separating the catalyst from the reaction medium by centrifugation and subjecting it to a drying it at 90 °C for 12 h. These authors obtained a good PV yield (41.5%) and GVL conversion (93.6%) during the first cycle after 12 h of reaction at 260 °C and 80 bar of H_2, due to the beneficial hydrogenation and the hydrophobic character of the HY zeolite in the octane solvent. However, they observed a lower performance in the second and third cycles, possibly due to the formation of coke and carbonaceous residues on the surface of the catalyst, obtaining a GVL conversion of 67.2%, a PV yield of 12.9% and PA yield of 10.5% in the third cycle. They also confirmed that the catalyst was stable under these reaction conditions, because the X-ray diffractograms of the fresh and spent catalyst showed similar phase structures, in agreement with the transmission electron microscopy (TEM) images that showed the absence of a noticeable change in the crystalline structure. However, larger Pd particle sizes in the spent catalyst after the third cycle were observed. In addition, they determined that the spent catalyst underwent pore expansion by means of N_2 adsorption-

desorption (BET) analysis. With regard to acidity, by temperature-programmed desorption of ammonia (TPD-NH₃), evident changes between the fresh and the spent catalyst were observed, which led the authors to conclude that there was a strong adsorption on the acid sites. Finally, Yan et al. carried out additional catalytic tests for the reuse of the catalyst, by calcination and subsequent reduction of the spent catalyst. In this way, they obtained a stable performance throughout several runs. In fact, in the fourth run they obtained a GVL conversion of 98.7% with a PV and PA yield of 45.7% and 41.0%, respectively. They also confirmed through characterization techniques (TEM and N_2 adsorption-desorption) that there was no change in structure and that the pore structure of the reduced Pd(5%)/HY catalyst used in the fourth run was comparable to that of the reduced fresh catalyst. Furthermore, they confirmed by XPS the absence of the oxidation state of PdO in the reduced Pd(5%)/HY catalyst. Additionally, they verified by analysing the reaction solution that there was no detectable leaching of Pd. It is worth mentioning that, though the authors employed the term "cascade upgrading of GVL" several times throughout the article, rigorously this process is based on orthogonal tandem catalysts, because more than one mechanism takes place over the bifunctional catalysts [45]. Finally, although this approach has the clear advantage of not requiring PL as reactant (PL was generated from the hydrogenolysis of PA), this process has other serious disadvantages such as: (a) using supported Pd catalysts with extremely high metal loadings (3-7%); (b) employing harsh reaction conditions (T > 250 °C and p_{H2} > 40 bar) and (c) utilizing octane as solvent, mainly produced from the petrochemical industry.

Novodárszki et al. studied the hydroconversion mechanism of GVL over two wide different catalysts: (a) Co(8%)/SiO₂ and (b) Pt(0.5%)/aluminosilicate catalysts in gas phase 250 °C, feeding H_2 at 3 L.h⁻¹ (pressure of 30 bar) and GVL with a WSHV of 1 $g_{GVL}.g_{cat}^{-1}.h^{-1}$ during 50 h, verifying that a significant deactivation did not take place over these samples [46]. However, the product distribution was markedly different. Over Co/SiO₂ the main products were 1,4-pentanediol (1,4-PD), 2-methyltetrahydrofurane (MTHF), 1-pentanol, 2-pentanol and butane, pentane, etc. as by-products, suggesting that the cleavage of the ester bond O(C=O) accounts basically for the adsorption of GVL over Co/SiO₂. In other words, the VE (or PA intermediate) formation was not promoted over Co/SiO₂ catalysts. In contrast, over Pt(0,5%)/H-MAG the main product was PA and PV was observed in minor amounts, confirming that ROUTE 1 (Figure 3) is promoted over this sample. By IR spectra of adsorbed pyridine, both Lewis and Brønsted acid sites of considerable acid strength were detected over Pt(0.5%)/H-MAG showing a Si/Al ratio of 19. In these conditions, the GVL conversion was 43.5% with a PA and PV selectivity of 91.7% and 7.6%, respectively, whereas to selectivities to MTHF and pentanols were lower than 0.4%. However, performing the reaction at 300 °C, the GVL conversion reached 90.2% and PA selectivity dropped to 79.4%, increasing the PV selectivity to 20.1%. Thus, the GVL interaction with the catalyst surface seems to take place through the (CH₃C)-O bond. The authors explained these differences in terms of the nature of the acid sites, considering that Co/SiO₂ only exhibited Lewis acid sites, whereas Pt/H-MAG showed both Lewis and Brønsted acid sites. In the case of Co/SiO₂, electronic structure calculations were included in the study to analyze the structure of adsorbed GVL. Even more, over Pt/H-MAG a strong hydrogen bond between GVL and strong Brønsted acid sites was evidenced by DRIFT

REVIEW

studies feeding GVL and H_2. Besides, by comparing the spectra of GVL over Pt/H-MAG and H-MAG authors concluded that the presence of small Pt particles does not significantly influence the GVL adsorption over acid sites. Finally, though the pentenoic acid intermediate was never detected, Novodárszki et al. agreed with other authors regarding that GVL ring-opening takes place over Brønsted acid sites via cracking of a protonated intermediate that leads to PA formation [35][36]. Even though this work tried to focus the study on the GVL hydroconversion mechanism over two widely different catalysts, it put some light on the acid requirements of the bifunctional catalysts for obtaining VE through ROUTE 1.

It is worth mentioning that, among the works where a minor production of VE has been observed following ROUTE 1 involving tandem catalysis, most of them only focused the efforts on obtaining PA from GVL or LA [31,47–51]. In these cases, the main purpose of the work was not related with the VE production, so, they were not considered for the analysis carried out in this review.

3.2.1.2. Use of non-noble metal-based catalysts

Apart from catalysts based on noble metals, certain authors have employed non-noble metal-based catalysts for producing VE or mixtures of VE and PA from GVL along ROUTE 1.

Wang et al. compared the catalytic performance of two Cu-based catalysts with 10 wt% of Cu deposited on HZSM-5 zeolite (Si/Al=100) [37]. Bifunctional catalysts were prepared by two different methods employing $Cu(NO_3)_2.3H_2O$ as precursor: (i) impregnation (Cu/HZSM-5) and (ii) in-situ hydrothermal crystallization method using CuO/SiO_2 particles as seeds (Cu@HZSM-5). The authors observed remarkable differences in both physicochemical properties and catalytic activity of the two samples Cu/HZSM-5 and Cu@HZSM-5. For instance, the Cu dispersion was five times higher in Cu@HZSM-5 (41.2%) than in Cu/HZSM-5 (8.0%), exhibiting an average metal particle size of 3.3 nm and 17.2 nm, respectively. Cu@HZSM-5 showed a higher reduction temperature suggesting a stronger metal-support interaction of the highly dispersed small Cu NPs. Regarding acidity, both samples desorbed NH_3 exhibiting two bands, one for weaker acid sites (150-400 °C) and the other for stronger sites (400-700 °C). For both samples, the temperature

at the maximum of the desorption peaks was higher than in the case of the bare HZSM-5, except for the weaker sites in Cu/HZSM-5 that remained equal. FTIR studies of pyridine preadsorbed indicated that the pattern for the L/(L+B) ratio was: HZSM-5 (0.65) < Cu@HZSM-5 (0.72) < Cu/HZSM-5 (0.96). Catalytic tests were performed using a fixed-bed reactor, at 300 °C, 10 bar of total pressure (H_2) and a WHSV of 0.6 h^{-1}. In these experimental conditions, the authors observed a modest GVL conversion (43.5%) for the bare HZSM-5, with a PA selectivity of 55.3%. In the case of the bifunctional samples, the GVL conversion was 98.5 and 72.1% for Cu/HZSM-5 and Cu@HZSM-5, respectively. However, the PA selectivity values were 35.5 and 94.5%, respectively. In all the cases the minority presence of 1-pentanol, 2-methyltetrahydrofuran, CO_2, CO and others was detected in the products. By using theoretical calculations, modelling the zeolite structure with 96 Si, 192 O atoms and using a 16 T HZSM-5 model and a Cu_4 cluster for the metal particles in both catalysts, the authors observed differences in the redistribution of transferred electrons in GVL from Cu. This resulted in a weaker C4-O1 bond strength versus C1-O1, implying that the C4-O1 bond scission takes place more easily. In summary, calculations results were in total agreement with those observed in the experiments, explaining the markedly different ring-opening mode of GVL over these Cu-based catalysts. Finally, the Cu@HZSM-5 sample proved to be efficient for producing EV from an ethanol solution of GVL (ROUTE 1 of Figure 5), reaching a combined PA and EV yield of 80%.

It is worth mentioning that Wang et al. had previously performed a study employing Cu/HZSM-5 catalysts prepared by wet impregnation using different Cu loading and Si/Al ratio in the support [52]. The catalyst with 10 wt% of Cu and Si/Al ratio equal to 15 exhibited a high catalytic activity and stability with 99.9% of GVL conversion and 85.3% of selectivity to C_{5+} hydrocarbons after 50 h of reaction at 325 °C, 20 bar (H_2) and a WHSV of 0.3 h^{-1}. Additionally, theoretical studies confirmed that the interfacial active sites between Cu and HZSM-5, involving uniformly dispersed Cu^0 and the acidic proton sites, promoted a unique spontaneous breaking of C1-O1 bond in GVL molecule to produce the pentene intermediate.

Also in 2022, Wang et al. reported the conversion of GVL employing two Co-based catalysts with 10 wt% of Co deposited on HZSM-5 zeolite (Si/Al=150) [38]. These bifunctional catalysts were prepared employing two different methods and using
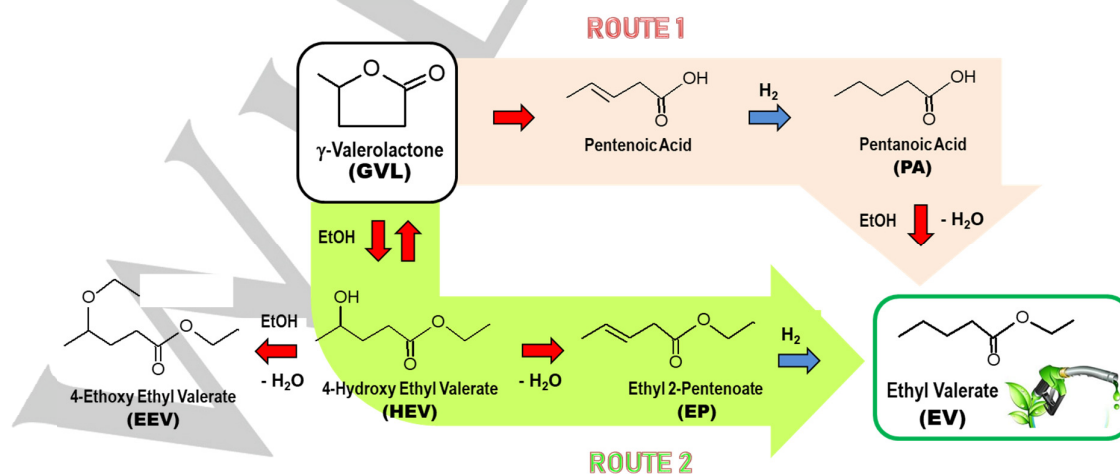

Figure 5: ROUTES 1 and 2 for the production of ethyl valerate (EV) from biomass-derived γ-valerolactone (GVL) involving multiple catalytic transformations (➡ acid-catalyzed reactions, ➡ metal-catalyzed reactions).

WILEY-VCH

$Co(NO_3)_2.6H_2O$ as precursor: (i) impregnation (Co/HZSM-5) and (ii) in-situ hydrothermal crystallization method using Co_3O_4/SiO_2 particles as seeds (Co@HZSM-5). Both catalysts presented significant differences regarding physicochemical properties and catalytic activity. The Co dispersion was higher in Co@HZSM-5 than in Co/HZSM-5, in agreement with the SEM and TEM analyses. Co@HZSM-5 exhibited a higher reduction temperature than Co/HZSM-5, suggesting a stronger metal-support interaction of Co-encapsulation structure. Concerning acidity, both samples desorbed NH_3 exhibiting two desorption peaks, corresponding to weaker acid sites (~300 °C) and stronger sites (~400 °C). Additionally, Co@HZSM-5 showed a peak around 720 °C that was attributed to the NH_3-desorption from Co species inside zeolite framework. For both bifunctional samples, the temperature at the maximum of the desorption peaks was higher than in the case of the bare HZSM-5, except for the weaker sites in Co@HZSM-5 that remained equal. A fixed-bed reactor was employed for the catalytic tests performed at 300 °C, 10 bar of total pressure (H_2) and a WHSV of 0.6 h^{-1}. For the bare HZSM-5, the GVL conversion was low (20.6%), though the PA selectivity was 60.2%. However, for the Co/HZSM-5 and Co@HZSM-5 bifunctional samples the GVL conversion reached 65.1 and 71.6%, respectively. However, the PA selectivity was markedly different, obtaining 11.0 and 98.7% for Co/HZSM-5 and Co@HZSM-5, respectively, because the former sample exhibited a high selectivity towards pentane (75.3%). Additionally, 1-pentanol, 2-methyltetrahydrofuran, CO_2, CO and others products were detected over this sample. In contrast, over Co@HZSM-5 only minor amounts of CO and others products were detected. Additionally, Co@HZSM-5 sample reached a combined PA and EV selectivity of 93.3% when an ethanol solution of GVL was fed to the reactor. Similarly to the previously commented work, the authors modelled the zeolite structure with 96 Si and 192 O atoms, using a 16 T HZSM-5 cluster model and Co_4 clusters for the metal nanoparticles. Theoretical calculations showed significant differences in the ring C-O bond strength of GVL, strongly suggesting a favourable valeric-oriented C4-O1 scission mode on Co@HZSM-5 and pentane-oriented C1-O1 scission mode of GVL ring-opening for Co/HZSM-5 sample, in total agreement with experimental results.

Previously, the same research group had performed a study combining experimental tasks and theoretical calculations for producing selectively pentane fuel from GVL over Co/HZSM-5 catalysts containing up to 20 wt% of Co and employing different Si/Al ratios in the zeolite support [41]. These authors reported an excellent catalytic performance of 99.9% GVL conversion with 93.5% selectivity to pentane fuel over Co(20%)/HZSM-5, using a fixed-bed reactor operated at 200 °C, 10 bar of total pressure (H_2) and WHSV of 0.3 h^{-1}, observing only traces of 1-pentanol, 2-methyltetrahydrofuran and others by-products. In particular, employing Co(5%)/HZSM-5 with Si/Al=80, they reached a 58.7% GVL conversion with a selectivity of 43.4, 31.6 y 9.7% to pentane, PA and PV, respectively. Both experimental and theoretical studies showed that the synergetic effect of interfacial active sites between metallic Co^0 and Brønsted sites of HZSM-5 is crucial for promoting the C1-O1 bond cleavage path of GVL toward the selective synthesis of pentane.

Finally, these authors also reported a flexible catalytic system comprising Ni as metal (deposited by wet impregnation) and HZSM-5 as acidic support for driving specific reaction paths towards either PA or pentane fuel with very high selectivity (97.3 and 93.6% respectively) [39]. Theoretical calculations (employing

similar metal clusters and unit cells than in the previously commented works) were in line with the experimental results, showing distinct redistribution of transferred electrons in GVL from two catalysts with different acidic properties due to the unlike Si/Al ratio. An increasing acidity (a lower Si/Al ratio) was responsible for a higher PA selectivity, providing a unique selectivity control, in contrast with reported Cu/HZSM-5 [40] and Co/HZSM-5 [41] catalysts showing only a mono-oriented selectivity ability.

Velisoju et al. explored the VE production in gas phase from GVL over promoted Ni(10%)/HZSM-5 catalysts, feeding a mixture of GVL (10 wt%) in EtOH and performing the reaction at 250 °C, with a GHSV of 0.54 mL.g_{cat}^{-1}.s^{-1} along with H_2 flow [53]. The metal promoters were Cr, Mo and W with a loading of 2 wt% and they were added in the final catalyst by co-impregnation with the $Ni(NO_3)_2$ precursor, whereas the support consisted of a HZSM5 zeolite with a Si/Al ratio of 40. Characterization results for the acid properties indicated that the total acid site density (determined by TPD-NH_3) followed the pattern: Mo-Ni/HZSM5 > W-Ni/HZSM5 > Cr-Ni/HZSM5, whereas the one for the Brønsted/Lewis ratio (estimated by FTIR of adsorbed pyridine) was: Mo-Ni/HZSM5 < W-Ni/HZSM5 $\cong$ Cr-Ni/HZSM5. Regarding the metal dispersion, the authors observed clear differences regarding the Ni specific surface area, showing the trend: Mo-Ni/HZSM5 < W-Ni/HZSM5 < Cr-Ni/HZSM5. The catalytic activity results showed relatively high EV selectivity (between 58.6 and 92.0%), but as the GVL conversion was intentionally kept below 10%, the EV productivity was relatively low, exhibiting values between 9.0 and 19.1 mmol EV.g_M^{-1}.h^{-1}. However, a very interesting section of this work was devoted to in situ FTIR studies during GVL adsorption and subsequent EtOH injection at 250 °C. Although the feeding of the EtOH and GVL was not simultaneous as in the catalytic tests, relevant remarks can be obtained from these studies. After GVL adsorption and feeding EtOH, the incipient formation of PA was observed and, after it, EV production. This is showing that the formation of PA intermediate depends strongly on the previous presence of GVL adsorbed on the catalyst surface instead of the alcohol. This is just the opposite of the situation in the case of VE production in liquid-phase processes, where the particular alcohol, playing both roles as reactant and solvent, is put in contact with the catalyst previously to the feeding of GVL. In these cases, PA intermediate is not observed, taking place the conversion of GVL along ROUTE 2. Interestingly, when Velisoju et al. fed GVL and EtOH at the same time to the continuous reactor, PA was formed with selectivity between 3.6 and 26.3% and minority products such as 4-hydroxy ethyl valerate (HEV), ethyl 2-pentenoate (EP) and 1,4-pentane diol (with a total selectivity between 3.7 and 15.1% depending on the promoter and the reaction conditions). These results strongly suggest that ROUTE 1 and ROUTE 2 (shown in Figure 5) take place simultaneously over these catalytic samples when GVL and EtOH are fed simultaneously. It is worth mentioning that this is the only work where intermediates of both ROUTES 1 and 2 were observed simultaneously.

Xu et al. studied the hydrogenation of GVL and LA over Cu-based catalysts in liquid phase, batch conditions, at 200 °C, 50 bar of H_2 and using EtOH as solvent [48]. The Cu catalysts had a metal loading of 30% and a wide variety of solids, from non-acidic such as SiO_2 to strong acidic such as HZSM-5, WO_3/ZrO_2, were employed as supports. Due to the fact that these authors explored the formation of many reaction products (MTHF, pentanol, pentanodiol, etc.) but the focus was not put on the VE

production, only the selectivity to the sum of EV and PA was reported. The highest productivity of the sum of PA and EV (1.5 mmol.g_{Cu}^{-1}.h^{-1}) was obtained over Cu-WO$_3$/ZrO$_2$, showing a selectivity of 53% but with a GVL conversion of 21% after 6 h. In this work, GVL and EtOH were contacted with the catalyst from the very beginning of the reaction, and thus, ROUTE 1 was promoted with the formation of PA and EV. The authors did not report the formation of intermediates of ROUTE 2 to EV, though the molar ratio EtOH/GVL employed in the catalytic tests was 34.3.

3.2.2. Valeric esters from GVL following ROUTE 2

3.2.2.1. Catalytic systems based on non-noble metal-based catalysts

As mentioned in section 3, ROUTE 2 for producing VE was reported by Chan-Thaw et al. where the conversion of GVL was carried out using alcohols as solvents [36]. These authors found that when the GVL conversion is performed in the presence of alcohols and acid catalyst, the ring-opening of GVL proceeds following a totally different mechanism from ROUTE 1. The whole mechanism involved in ROUTE 2 is shown in Figure 3 and described in section 3.2 for the case of the production of PV. Following ROUTE 2, Chan-Thaw et al. studied not only the production of PV but also ethyl valerate (EV), using in the latter case EtOH instead of PL as reactant and solvent. On the one hand, when EtOH was used, the reaction products were (Figure 5): 4-hydroxy ethyl valerate (HEV), ethyl 2-pentenoate (EP), 4-ethoxy ethyl valerate (EEV) and ethyl valerate (EV). Catalysts tested were based exclusively on Cu and supported on amorphous weakly acidic material such as SiO$_2$-ZrO$_2$, with ZrO$_2$ content of 4 and 4.7 wt.%, Cu loading of 5 and 8 wt.% and prepared by chemisorption-hydrolysis method. The authors claimed that the presence of Lewis acid sites plays an essential role in promoting the opening of the GVL ring. Catalytic tests were carried out at 250 °C, 10 bar of H$_2$, 700 rpm, GVL/catalyst ratio of 10:1 (by weight) and GVL/alcohol ratio of 1:10 (molar) and reaction time of 20 h. In the case of the reaction between GVL and EtOH, the best results in terms of selectivity were achieved over Cu(8%)/SiO$_2$-ZrO$_2$ with 4.7 wt.% of ZrO$_2$, reaching a GVL conversion of 69% with a selectivity to EV and EEV of 59 and 31%, respectively, without detecting EP, suggesting that the catalyst show a relatively high hydrogenation capacity. Using a lower ZrO$_2$ content it was possible to reach a higher conversion (X_{GVL}=77%) with selectivity to EV and EEV of 37 and 56%, respectively. For the sake of comparison, a Cu(8%)/SiO$_2$-Al$_2$O$_3$ catalyst was also tested and a conversion of 77% was obtained, as well. However, due to the lower reducibility of Cu over this support, a minor fraction of Cu atoms was reduced in the activated sample, leading to a selectivity of EV, EEV and EP of 32, 39 and 22%, respectively. When a Cu(5%)/SiO$_2$-ZrO$_2$ was used, these values of selectivity were 44, 36 and 18%, respectively, with a final GVL conversion of 67%. On the other hand, when the conversion of GVL was performed in the presence of PL, the GVL conversion and PV selectivity were markedly higher. Over Cu(8%)/SiO$_2$-ZrO$_2$ a GVL conversion of 93% was achieved after 20 h, with a selectivity to PV and PPV equal to 59 and 21%, respectively. Besides, the authors proved the effect of reducing the PL/GVL ratio up to a value of 5, observing that these selectivities changed into 72 and 16%, respectively, i.e. the formation of PPV diminishes when the PL/GVL ratio decreases, in agreement with an etherification

reaction. Finally, recycle tests were carried out for both systems, observing a slight increase in the EV and PV selectivity, keeping almost constant the GVL conversion with the runs. In the case of using EtOH, after the 5th run a 57% of GVL conversion with a EV yield of 40% were reached, giving a EV productivity of 25.4 mmol.g_{Cu}^{-1}.h^{-1}. For the production of PV, after the 4th run they reached a X_{GVL}=90% with selectivity to PV of 83%, leading to a PV productivity of 47.7 mmol.g_{Cu}^{-1}.h^{-1}. The authors reported that although PA was not detected in the reaction mixture, the formation of PA can not be excluded because in these experimental conditions with excess of PL it would be readily esterified to PV. In other words, the main intermediate of ROUTE 1 was not observed and the VE formation took place mainly along ROUTE 2, with the formation of different reaction intermediates. In summary, this alternative reaction path to that reported by Lange et al. meant a significant improve in terms of selectivity to the desired VE, especially in the case of PV. Besides, this work was the first report of the study of the valeric esters production in a batch one-pot process involving orthogonal tandem catalysts carried out by a weakly acidic amorphous material combined with a relatively cheap hydrogenation metal. Last, but not the least, it should be noted that the authors did not report the Cu leaching phenomenon during PV production, but this undesirable process took place during the EV production, fact verified through ICP analysis of the reaction mixture.

Based on the work of Chan-Thaw et al., Scotti et al. prepared catalysts by chemisorption-hydrolysis in order to investigate the role of low coordination sites in SiO$_2$-supported Cu catalysts in the conversion of GVL in the presence of PL and H$_2$, for producing PV [54]. The Cu loadings were between 9 and 15% and two commercial SiO$_2$ supports with different textural characteristics were used: SiO$_2$ A (S_g=413 m^2/g, V_P=0.75 cm^3/g and D_P=72 Å) and SiO$_2$ B (S_g=693 m^2/g, V_P=0.62 cm^3/g and D_P=36 Å). These samples were tested at 250 °C, 10 bar of H$_2$ and 690 rpm for 10 h, with a PL/GVL molar ratio of 5 and 400 mg of catalyst. With the Cu(12%)/SiO$_2$ B catalyst, which exhibited the highest density of Lewis acid sites, a PV selectivity of 92% with a GVL conversion of 91% was obtained. On the other hand, the catalysts prepared on SiO$_2$ A and the unreduced CuO(12%)/SiO$_2$ B were less active, reaching a GVL conversion of 81% and a PV selectivity with the Cu(15%)/SiO$_2$ A of 70% and with the CuO(12%)/SiO$_2$ B catalyst a GVL conversion of 83% and selectivity to PV of 65%. In contrast, when the bare support SiO$_2$ B was tested, a GVL conversion of 7% and a PPV selectivity of 57% was attained, which was improved when SiO$_2$-ZrO$_2$ was tested, evidencing the relevant role of the Brønsted acid sites in this reaction mechanism. Regarding the particular role of acidity, these authors carried out an exhaustive investigation on the acidity of the Cu(12%)/SiO$_2$ B catalyst by means of FT-IR of adsorbed pyridine and by titration with 2-phenylethylamine in cyclohexane. Using these techniques, they verified that the reduction of the CuO phase to the metallic state increases the acidity of the material. In fact, based on the results obtained in the titrations, the authors claimed that SiO$_2$ B presented the highest total acid site density and a stronger acid sites density than the Cu(9%)/SiO$_2$ B and Cu(12%)/SiO$_2$ B catalysts, due to its larger surface area. However, the proportion of strong to total acid sites followed the pattern: SiO$_2$ B (52%) < Cu(9%)/SiO$_2$ B (60%) < Cu(12%)/SiO$_2$ B (71%). Regarding the acid strength, they observed the same pattern: SiO$_2$ B < Cu(9%)/SiO$_2$ B < Cu(12%)/SiO$_2$ B. By high-resolution transmission electron microscopy (HRTEM) of the Cu(12%)/SiO$_2$
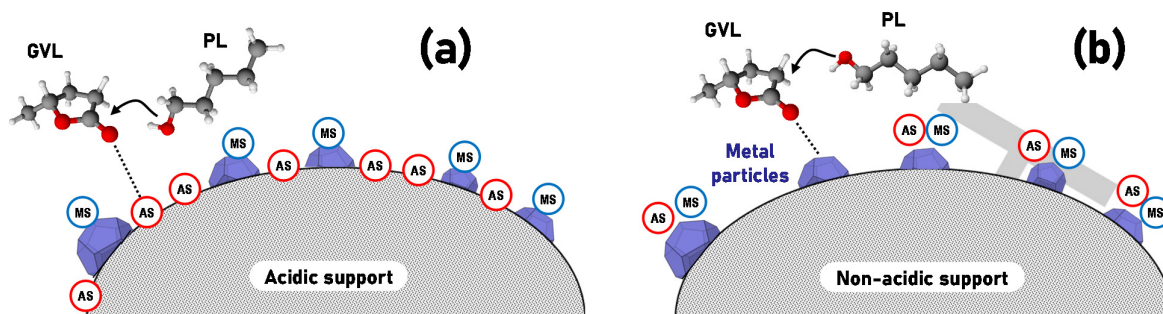
Figure 6: Ring-opening of γ-valerolactone (GVL) with pentanol (PL) for the production of pentyl valerate (PV) following ROUTE 2 over: (a) a bifunctional acid/metal catalyst prepared by depositing a metal over an acidic support and (b) a bifunctional acid/metal catalyst prepared by depositing metal particles over a non–acidic support where metal particles also promote the acid-catalyzed steps (AS acid sites, MS metal sites).

B catalyst, well-dispersed spherical nanoparticles were observed on the support, with an approximate particle size of 4.7 nm. The authors demonstrated that these particles not only have a relevant role in the hydrogenation reaction, but also in the activation of the GVL towards the nucleophilic addition of PL due to their Lewis acid properties. Analysis of the IR spectra of adsorbed GVL revealed that when Cu is present on SiO_2 there is a strong chemisorption of the reagent through the C=O double bond. Therefore, it was proposed that the presence of a single catalytic site and the absence of catalytically relevant Brønsted acid sites on the support may have a positive effect on PV selectivity. In other words, the authors showed that very small metal particles can also exhibit catalytically significant Lewis acidity, which helps to activate the GVL molecule on the surface. This property, together with an important metal hydrogenation activity, allowed them to design a new bifunctional catalyst (Cu/SiO_2), without the need of an acid support. In the case of the GVL conversion to PV, this led to not only a simpler catalytic system, but also to a more selective one.

It is worth noticing that the works of Chan-Thaw et al. and Scotti et al. followed two totally different approaches for providing acidity to the bifunctional catalysts. These two alternatives are shown in Figure 6. The first approach (Figure 6.a) involves the use of an acidic support (e.g. SiO_2-ZrO_2) where metal particles were deposited by chemisorption-hydrolysis. The second approach, using the same preparation method and a non-acidic support (SiO_2) allows obtaining metal particles that provide both metal and Lewis acid sites (Figure 6.b). This second approach requires a fine tuning of the morphology of the metal particles to increase the acid site density. In contrast, the first approach allows a wider range of options for selecting the acid and metal function, though some interaction between metal and acid sites can take place modifying the acid/metal balance.

In 2014, Sun et al. studied the conversion of LA and GVL in the presence of ethanol into EV [55]. They compared the performance of a Co/HZSM-5 catalyst, prepared by incipient wetness impregnation of commercial HZSM-5 zeolite (Si/Al=38) with $Co(NO_3)_2 \cdot H_2O$, with another catalyst based on cobalt nanoparticles embedded in HZSM-5 crystals (Co@HZSM-5), the latter obtained by an in situ synthetic strategy using Co_3O_4/SiO_2 as the precursor for the nucleation and growth of HZSM-5 crystals. Although both catalysts showed a very similar metal loading (10%wt.), Co@HZSM-5 exhibited much smaller Co particles (15 ± 1 nm) than Co/HZSM-5 (25 ± 3 nm). The catalytic tests were performed at 240 °C, 30 bar of H_2, using 6 mL of ethanol and 1.0 g of LA or GVL. Although this work was mainly focus on the production of EV from LA and the synthesis of a

robust catalyst to avoid the sintering and leaching in the presence of LA, a particular run was carried out using GVL as reactant that deserves to be mentioned. After 3 h, over Co/HZSM-5 a GVL conversion of 93% was attained with selectivity to PA and EV of 22 and 69%, respectively. The presence of PA in the reaction mixture indicated that over Co/HZSM-5 not only ROUTE 2, but also ROUTE 1 was promoted in a certain degree. However, when only HZSM-5 was used, a GVL conversion of 45% was attained with an ethyl pentenoate yield of 45%. These results strongly suggest that the first reaction between GVL and the alcohol is a reversible reaction and if there is not a consumption of ethyl pentenoate by hydrogenation, the equilibrium is not shifted towards a high GVL conversion. Besides, no PA was observed due to the fact over the bare acidic HZSM-5 sample ROUTE 1 is not promoted if the metal catalytic function is not present. Finally, it is worth mentioning that the embedded catalyst Co@HZSM-5 was not tested using GVL as reactant, so the comparison of the performance of this sample with that of Co/HZSM-5 in the GVL conversion can not be done.

In 2017 Li et al. synthesized Cu/ZrO_2-$ZnAl_2O_4$ (Cu/ZZA-x) catalysts by the urea-assisted precipitation method with a 10 wt% Cu loading and with different $[Zr^{4+}]/[Zn^{2+}]$ molar ratios (x=0, 0.1, 0.2 and 0.3) [56]. These catalysts were used in the catalytic transformation of GVL in the presence of PL at 250 °C, 10 bar of H_2, 1000 rpm, with a catalyst mass of 0.4 g, 4.0 g of GVL and 20 mL of pentanol for 10 h. In these tests, the Cu/ZZA-0.2 catalyst presented the highest conversion of GVL with a value of 91% and a PV selectivity of 99%, which was correlated with a higher dispersion of Cu since more Cu^+ species can be formed on the surface due to the strong interactions with the support. In this sense, the higher the Zr content, the higher the Cu dispersion and the acidity, as well. In contrast, lower GVL conversions (<70%) with slightly lower PV selectivity were obtained over other Cu catalysts supported on ZnO, Al_2O_3 or ZrO_2. Additionally, the catalytic activity of the Cu/ZZA-0.2 catalyst was tested in different alcoholic solvents (methanol, ethanol, propanol and butanol) and in all cases it was found that the yields of the corresponding valeric esters were greater than 90%. The authors also studied the stability of the Cu/ZZA-0.2 catalyst through reuse tests, confirming that the PV yield decreases only 5% after four consecutive catalytic cycles. The structural characterization of the spent catalyst showed that the porous structure does not change after the four reaction cycles and agglomeration of Cu particles does not take place. These authors also carried out additional tests to investigate the role of the nature of acidity. In the first, pyridine was added to the

reaction mixture to block Lewis and Brønsted acid sites, while in the second, 2,6-dimethylpyridine was added to block only the Brønsted sites. The results of the tests reflected the relevance of the different surface acid sites. Thus, the GVL conversion decreased greatly when the sites were inactivated with pyridine, also observing a lower amount of PA formed after 10 h of reaction due to selective inhibition of the Brønsted acid sites. This is in agreement, to a certain extent, with the results of Scotti et al. [54], who verified that the Lewis sites are key for the opening of the GVL ring with PL. Besides, Li et al. studied the effect of metal sites by preparing Cu/ZZA-0.2 catalysts with different Cu loadings, specifically, 3.26, 6.53, and 13.1 wt%. In all cases, they showed that after 10 h of reaction both the GVL conversion (12, 18 and 23%, respectively) and PV selectivity (68, 80 and 82%, respectively) increased for a larger Cu loading. However, the PP and PPV selectivity increased notably for Cu loads lower than 9.8%, attributed to the decrease in the amount of active metal sites on the surface. In addition, these authors obtained a higher selectivity to PA when the copper load increased from 9.8 to 13.1%, due to the existence of more active metallic sites in Cu/ZZA-0.2 promoting also ROUTE 1. Thus, these authors proposed that both reaction pathways (ROUTE 1 and 2) are possible by virtue of the types of acid sites on the Cu/ZZA catalyst surface, which promote PV production. In the first case, protonation can take place to open the GVL ring and form pentenoic acid in the presence of the Brønsted sites, followed by esterification with PL and hydrogenation to produce PV (ROUTE 1). In contrast, Lewis acidic sites activate the C=O bond in the GVL molecule via the oxygen lone pair, leading to ring opening by direct nucleophilic addition of PL to the carboxylic group (ROUTE 2). In addition, electrophilic centers Cu^+ species on the surface can facilitate the polarization of the carboxylic group to a certain extent. In summary, very high GVL conversion and PV yield were attained with $Cu/ZrO_2-ZnAl_2O_4$, though a relatively complex preparation method was used.

Also in 2017, Liu et al. employed Cu/ZrO_2 catalysts in the PV production from GVL, PL and H_2, developing a CuO/ZrO_2 precursor with uniformly distributed Cu and Zr [57]. These catalysts were prepared by separate nucleation and aging steps, assisted by reduction-oxidation strategies using $NaBH_4$. Different initial molar ratios of $NaBH_4/(Cu+Zr)$ (x=10, 15, 20, 25) and Cu loadings between 9.5 and 9.9% were used. These authors claimed that the homogeneous dispersion of CuO, the high surface area of the support (ZrO_2) with a controlled porous structure and a strong interaction between CuO and ZrO_2 in the CuO/ZrO_2 precursor could lead to a greater dispersion of the Cu and the formation of Cu^+ active sites. These catalysts were tested at 230 °C, 15 bar of H_2 and 10 h. Among the series of Cu/ZrO_2-x samples, the Cu/ZrO_2-20 catalyst showed the best catalytic performance (85.4% GVL conversion and 98.0% PV selectivity) and the highest initial GVL conversion rate. The value of r^0_{GVL} increased following the pattern: Cu/ZrO_2-25 < Cu/ZrO_2-10 < Cu/ZrO_2-15 < Cu/ZrO_2-20. In addition, catalysts prepared by co-precipitation (CP) and chemisorption-hydrolysis (QH) methods were tested in the same conditions. GVL conversion and PV selectivity with Cu/ZrO_2-CP and Cu/ZrO_2-QH were much lower than on the Cu/ZrO_2-x catalysts. The lower catalytic performance of the Cu/ZrO_2-CP and Cu/ZrO_2-QH catalysts was attributed to the low Cu dispersion, which may be due to a poor interaction between CuO and the ZrO_2 support and the high mobility of the active Cu species in the CuO/ZrO_2-CP and CuO/ZrO_2-QH precursors during the reduction step. The authors also employed other oxides (SiO_2, MoO_3 and Al_2O_3) as

support to prepare Cu-based catalyst by chemisorption-hydrolysis method, observing that the conversion of GVL and the PV selectivity were lower than the Cu/ZrO_2-QH catalyst. Based on these results, the authors affirmed that the high dispersion of the Cu nanoparticles and the cooperation of the Cu^0 and Cu^+ surfaces are crucial to achieve a high catalytic performance in the transformation of GVL under these experimental conditions, not being the surface acidity a dominant factor in this case. Finally, these authors proposed a possible mechanism for the catalytic transformation of GVL with PL and H_2 on Cu/ZrO_2 catalysts. Firstly, the C=O bond of GVL can be adsorbed and polarized by electrophilic Cu^+ species on the surface, favoring the nucleophilic addition of the electronegative hydroxyl group of PL, leading to the formation of the HPV intermediate. Secondly, PP can be formed sequentially by the rapid dehydration of HPV. Finally, the highly dispersed Cu^0 active centers on the surface are responsible for dissociating H_2 to produce active hydrogen for the final hydrogenation of PP to PV. Indeed, the cooperation between highly dispersed Cu^+ and Cu0 species on the surface gives the Cu/ZrO_2 catalyst prepared by Liu et al. a remarkable catalytic performance in the transformation of GVL to PV. Additionally, the use of different alcohols (methanol, ethanol, propanol, butanol, pentanol, hexanol, cyclohexanol, isopropyl and isoamyl alcohol) and their application in the preparation of various alkyl valerates was explored, finding that the conversion of GVL decreases as the hydrocarbon chain of the primary alcohol increases. Finally, reusability tests for the Cu/ZrO_2-20 catalyst were carried out, observing a slightly lower catalytic performance (80.0% GVL conversion and 97.6% PV selectivity) after four catalytic cycles. The authors attributed the slight decrease in the performance after four catalytic cycles to the leaching of Cu.

In 2020, our group reported the catalytic performance of Ni-based catalysts supported on $SiO_2-Al_2O_3$ (SA) in the GVL conversion into PV in the presence of PL and H_2, comparing two catalysts prepared by incipient wetness impregnation (I) and precipitation-deposition (PD) with approximately the same metal loading (8%) [58]. Important differences in terms of both acidity and metal dispersion were observed over these samples. The total acid site density determined by $TPD-NH_3$ was 0.60 and 0.31 $\mu mol/m^2$ for Ni/SA-I and Ni/SA-PD, respectively. In the case of the Ni dispersion the values were 5 and 12%, respectively. These samples also exhibited different values of H_2 chemisorption capacity, with values of 2.7 and 4.0 $Ncm^3.g_{Ni}^{-1}$ for Ni/SA-I and Ni/SA-PD, respectively. The catalytic tests were carried out at 250 °C, 10 bar of H_2, using 1.5 ml of GVL, 40 ml of PL and 0.25 g of catalyst. Both catalysts were active in these experimental conditions, though Ni/SA-I was markedly more active than Ni/SA-PD. For the latter, the initial GVL conversion rate was $r^0_{GVL}=3.66\times10^{-3}$ $mol.g_{cat}^{-1}.h^{-1}$, whereas for the former was $r^0_{GVL}=2.39\times10^{-2}$ $mol.g_{cat}^{-1}.h^{-1}$. The GVL conversion after 8 h over Ni/SA-PD was 40.9% with a PV yield of 29.3%, showing a PV selectivity of about 71.6% and a carbon balance of 99.9%. In contrast, with Ni/SA-I a GVL conversion of 67.0% was reached after 8 h, with a PV yield of 55.1%. With these values, the PV selectivity was 82.2% and the carbon balance was equal to 99.5%. It is worth mentioning that PA was detected (3 mol%) in the reaction mixture when Ni/SA-I was used, indicated that ROUTE 1 was also promoted over this catalyst but in a much lower degree that ROUTE 2. In contrast, with Ni/SA-PD only ROUTE 2 was favored and no PA formation was observed. TOF values (based on the acid site density) were 113.8 and 32.3 h^{-1}

for Ni/SA-I and Ni/SA-PD, observing that the former value was very similar to the TOF determined over the bare SA support (with an acid site density of 0.59 µmol/m^2). Finally, with Ni/SA-I a re-use test comprising three catalytic cycles of 7 h was performed in order to verify whether some deactivation process takes place. The GVL conversion diminished from 75.2% in the first reaction cycle to 59.2% in the third cycle. The drops for PV yield and PV selectivity from the first cycle to the third were about to 30.2% and 28.6%, respectively, verifying by ICP that leaching of Ni was not the cause of this phenomenon. In summary, although the GVL conversion and PV selectivity attained in this work were not higher than the observed with Cu-based samples, this was the first work using Ni-based catalysts and where the effect of the preparation method on the catalytic performance for producing PV following ROUTE 2 was studied. Thus, it was concluded that precipitation-deposition (PD) method, leading to a higher Ni dispersion, reduces significantly the acid site density in bifunctional Ni/SA-PD catalyst and consequently the catalytic performance in comparison to a catalyst prepared by incipient wetness impregnation, where the acid site density of the support is not markedly modified.

3.2.2.2. Bifunctional catalysts based on noble metals

The first study of the production of VE following ROUTE 2 involving noble metal-based catalysts was reported by Zhang et al. in 2014 [59]. These authors studied the conversion of GVL in the presence of ethanol into EV employed Pd nanoparticles supported on sulfonic acid functionalized MIL-101. First, they studied the influence of HSO$_3$ content on the acidity of the support. In this sense, they synthesized the MIL-101-SO$_3$H(x) supports, in which x is the proportion of monosodium 2-sulfoterephthalic acid in the synthetic solution. The first catalytic tests were performed at 200-250 °C, 30 bar of N$_2$, using 5.82 mL of ethanol and 10 mmol of GVL into a stainless-steel batch reactor. With unmodified MIL-101, GVL conversion was around 3.1% and 4-hydroxy ethyl valerate (HEV) was the only product. On the other hand, the GVL conversion for MIL-101-SO$_3$H(25) was higher at 7.8%, indicating that the Brønsted acid SO$_3$H groups are in some way involved in the first acid-catalyzed reaction. Even more, for samples with higher SO$_3$H loading, it was seen that ethyl 2-pentenoate (EP) was formed in greater amounts at the expense of HEV, showing the importance of Brønsted acidity on the second acid-catalyzed reaction. When the MIL-101-SO$_3$H(100) sample was run at 250 °C, EP was the main product with a selectivity of 90% at a GVL conversion of 86%. After selecting the best support, these authors studied the one pot conversion of GVL over Pd/MIL-101-SO$_3$H(100) at 200-250 °C, 30 bar of H$_2$, using 10 mmol of GVL, 5820 µL ethanol and 0.25 g of catalyst. Pd(5%)/MIL-101-SO$_3$H(100) showed the highest GVL conversion among the catalysts, reaching a GVL conversion of 51% with selectivity to HEV and EV of 66 and 26%, respectively after 10 h. When the Pd loading was 1 and 2.5 wt%, the selectivity of EV was only 15 and 20%, respectively. At 250 °C, 30 bar of H$_2$ and using 5 wt% Pd(5%)/MIL-101-SO$_3$H(100) as catalyst a GVL conversion of 98% and a EV yield of 83% were obtained. It is worth mentioning that the highest EV productivity attained was 166.0 mmol.g$_M^{-1}$.h^{-1}. Finally, the stability of the catalyst was investigated, finding that GVL conversion dropped by 10% after each run. Moreover, the EV yield decreased remarkably during the second run, showing clearly that the Pd nanoparticles strongly deactivated after one run.

With the motivation of increasing the PV productivity in batch one-pot processes before moving to continuous processes, our group prepared by incipient wetness impregnation SiO$_2$-Al$_2$O$_3$-supported Ru, Ir and Pt catalysts (M/SA) with a moderate metal loading (1%) and tested them in the PV production from GVL, PL and H$_2$ in a one-pot process [60]. These catalysts were prepared using chlorinated precursors of Ru, Ir and Pt. Characterization results indicated that the Cl content (coming from this metal precursor) followed the pattern: Ru/SA >> Ir/SA > Pt/SA. The pattern for the average size of metal particles was: Ru/SA (7.4 nm) > Ir/SA (6.7 nm) > Pt/SA (2.8 nm). Regarding acid properties, the surface acid site density (n$_A$) followed the pattern: Pt/SA (0.86 µmol/m^2) > Ir/SA (0.65 µmol/m^2) > SA (0.59 µmol/m^2) > Ru/SA (0.52 µmol/m^2). The nature of these acid sites was determined by FTIR of chemisorbed pyridine, resulting the following pattern for the L/(L+B) ratio: SA > Pt/SA $\cong$ Ir/SA > Ru/SA, showing the Ru/SA sample a value 17% lower than SA support. It is worth mentioning that the higher the chlorine content, the lower the L/(L+B) ratio of the samples. Regarding the catalytic tests, the GVL conversion over Ru/SA and Ir/SA after 8 h (60.6% and 57.7%, respectively) was not significantly higher than the value obtained over SA support in the absence of metal and H$_2$ (55.5 %). This strongly suggested a lower hydrogenation capacity of Ru/SA and Ir/SA for converting PP into PV. It was determined, based on the values of the ratio between the initial GVL moles and the amount of acid sites (n°$_{GVL}$/(n$_A$.S$_g$.W$_c$)=294, 233 and 171 for Ru, Ir and Pt, respectively, Ru/SA and Ir/SA) that the catalyst surface worked at a very high coverage in all the samples. The final yield of the undesirable product PPV at 8 h was between 10 and 14.3% for the three M/SA catalysts, indicating that the undesirable acid-catalyzed reaction HPV + PL $\Rightarrow$ PPV + H$_2$O is not strongly influenced by the acid site density and/or metal dispersion. After 8 h, the sum of the PP and PV yield was equal to 20.5, 26.2, 36.8 and 54.0% for SA, Ru/SA, Ir/SA and Pt/SA, respectively. This is showing that the orthogonal tandem involving the dehydration of HPV into PP and the subsequent PP hydrogenation into PV was promoted following the pattern: Pt/SA > Ir/SA > Ru/SA > SA. The better catalytic performance of Pt/SA was explained considering not only that each acid site must convert a significantly lower amount of GVL molecules on Pt/SA than on Ru/SA and Ir/SA, but also the fact that Pt/SA catalyst has smaller metal particles that promotes more efficiently the H$_2$ chemisorption and PP hydrogenation. Besides, the chlorine residues modify the density and nature of surface acid sites leading to a lower C balance and a higher TOF over Ru/SA than over Ir/SA and Pt/SA, suggesting that a stronger GVL adsorption diminishes PV productivity. Besides, the action of residual chlorine on the -OH groups of SA can create a new kind of acid sites, reducing the H$_2$ chemisorption capacity of the metal particles by electronic effects. In summary, Pt/SA with the highest acidity and metal dispersion of the series was the best catalyst for the PV production from GVL, PL and H$_2$, and additional experiments varying the mass of catalyst were carried out over this sample in order to improve PV productivity. The best catalytic performance was obtained after 10 h and using 0.5 g of catalyst, keeping constant the rest of the reported experimental conditions, where a final GVL conversion of 100% and a PV yield and selectivity of 90.0% were attained. In these conditions a PV productivity of 300.1 mmol.g$_M^{-1}$.h^{-1} was obtained. With all this knowledge and, with the aim of improving the PV productivity even more, our group prepared, characterized and tested SiO$_2$–Al$_2$O$_3$-supported Rh and Pd-based bifunctional

catalysts with relatively low metal loading ($\cong$1 wt%) [61]. The M^0/SA catalysts exhibited a specific surface area and pore volume slightly lower than those of the SA support and the presence of metal nanoparticles with an average size of 5.6 nm for Rh/SA and 3.7 nm for Pd/SA. Regarding acid properties, a total acid site density 45% higher than that of SA was determined for Pd/SA, whereas a value 10% lower was observed for Rh/SA. The relative strength of acid sites followed the pattern: Pd/SA > Rh/SA > SA with mainly Lewis acid sites in all the cases. Regarding the catalytic tests, Pd/SA catalyst, without chlorine residues from the metal precursor, with a higher surface density of acid sites, higher acid strength and smaller metal particles, was more active and selective than Rh/SA, reaching a GVL conversion of 81.1% and a PV yield of 70.1% after 8 h. Indeed, Pd/SA was the best catalyst for the production of PV from GVL, PL and H_2. The basic parameters of a pseudo-homogeneous kinetics with the best catalyst (Pd/SA) were a reaction order for H_2 of about zero, a unitary reaction order in the case of GVL and apparent activation energy of 25.6 kcal.mol^{-1}. Besides, reusability tests for the Pd/SA were carried out, observing that the catalytic performance dropped significantly from the 2nd to the 3rd run, with a lower deactivation from the 1st to the 2nd run. However, no leaching process took place over the Pd/SA catalyst. This is a clear advantage over Cu-based catalysts, where significant leaching was reported [36]. Based on the information provided by TPO profiles it was assumed that the regeneration procedure employed between catalytic cycles eliminated almost completely the carbonaceous deposits from the catalytic surface. Considering the previous results, the cause of the deactivation of Pd/SA might be ascribed to a sintering process. Finally, the PV productivity values per gram of metal obtained over Rh/SA and Pd/SA in this work (376.5 and 660.7 mmol $g_M^{-1}.h^{-1}$) were the highest values reported for the PV production in a one-pot process, as Table 1 shows.

3.2.2.3. The paramount importance of acidity

To put some light on the acidity necessary to carry out the orthogonal tandem catalysis along ROUTE 2, our group performed a particular study about the specific role of the acid sites on the conversion of GVL with PL to PP focusing the attention on the two-consecutive acid-catalyzed reactions: (1) nucleophilic addition of PL to GVL to form HPV and (2) HPV dehydration into PP [62]. Solids covering a wide range of textural and acidic properties were tested, from non-acidic ones such as SiO_2 to strongly acid solids with different acid site density, strength and nature, such as γ-Al_2O_3, ZnO/SiO_2, HPA/SiO_2, and NaY, HY, HMOR zeolites. The catalytic tests of GVL conversion with PL were carried out in liquid phase at 250 °C, 10 bar of N_2, 0.25 g of catalyst, 40 ml of PL and an initial GVL concentration of 0.37 M. The catalyst activity and selectivity strongly depended on: (i) the nature; (ii) strength and (iii) density of acid sites of the solid. Samples containing predominantly Lewis acid sites, such as ZnO/SiO_2, γ-Al_2O_3 and NaY zeolite promoted mainly a strong GVL adsorption leading only to a relatively high missing carbon balance. HPA/SiO_2 having mainly surface Brønsted acid sites of medium–high strength showed a very high activity and selectivity to PP but deactivated dramatically due to severe leaching in PL. Zeolites containing at least 40% of Brønsted acidity and strong acid sites promoted remarkably the undesirable intramolecular dehydration of pentanol into pentenes. On the other hand, SiO_2-Al_2O_3, exhibiting a B/(L+B)

ratio of 0.21 and a wide strength of acid sites, was more selective to PP than to PPV, though the missing carbon balance was relatively high. By calorimetric adsorption and temperature-programmed oxidation, adsorption enthalpies of 61.9 and 59.1 Kcal.mol^{-1} for GVL and PL were determined, respectively. Besides, by temperature-programmed desorption experiments it was concluded that GVL adsorption is irreversible on SiO_2-Al_2O_3, whereas in the case of PL is partially reversible. The effect of the calcination temperature on the product distribution and evolution of the missing carbon balance was also studied over SiO_2-Al_2O_3. Based on our results over noble metal-based catalysts [60][61], a particular correlation between the Lewis proportion of the strong acid sites (outgassing the pyridine at 450 °C) and the PV selectivity (at X_{GVL}=50%) was observed, as Figure 7 shows. This is indicating that the strength of Lewis acid sites is relevant for the two acid-catalyzed reactions. Data in Figure 7 exhibits a clear tendency between a higher proportion of Lewis nature in the stronger sites and a higher selectivity to PV. In other words, it is observed that on Pd/SA, Pt/SA and Rh/SA the acid function promoted the desirable reactions to a greater extent than on Ir/SA and Ru/SA. Particularly, on the Pd/SA the fraction of Lewis sites among the strong acid sites was the highest. These sites seem to be an important factor in the GVL conversion to pentyl valerate, which is in agreement with the results of other authors [36][54].

It deserves to be mentioned that Lange et al. also tested ROUTE 2 for the particular case of the production of methyl pentenoate, a promising biomass-derived Nylon intermediate, from GVL and methanol under catalytic distillation conditions in 2007 [63]. It is interesting to note that this work was published six years before the work of Chan-Thaw et al. [36], but with a clearly different motivation, producing methyl pentenoate instead of methyl pentanoate biofuel. This process was based on the large difference in boiling point between GVL and methyl pentenoate to shift the thermodynamic equilibrium towards the desired product. The reaction was conducted in fed-batch mode because the GVL was initially loaded in a distillation flask (operating also as reactor) with the acid catalyst, whereas the methanol was continuously fed. The distillate product, consisting of methyl pentenoate, unconverted methanol and water was continuously removed using a rectification column. Different acid catalysts were tested, from homogeneous catalysts such as H_2SO_4, p-toluene sulfonic acid (pTSA) and La(OTf)$_3$ to
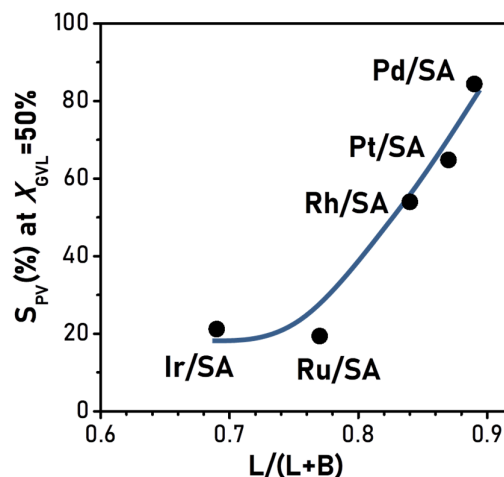

Figure 7: Selectivity to PV vs. Lewis proportion of strong acid sites on noble metal-based catalysts tested in ROUTE 2.

heterogeneous ones as Nafion NR50, HZSM-5, HBEA zeolites, SiO_2-Al_2O_3, Al_2O_3, La(16%)/Al_2O_3 and KOH. The reaction was performed at a temperature of 200 °C, with a catalyst loading between 1 and 7 wt% and a methanol feed rate equal to 0.23 $mol_{GVL}^{-1}.h^{-1}$. All catalysts (homogeneous and heterogeneous) exhibited some activity in the reaction, being the most initially active H_2SO_4 and followed by pTSA. For the solid catalysts, the initial activity decreased in the pattern of the acid strength: Nafion NR50 > zeolites > SiO_2-Al_2O_3. When pTSA is used as homogeneous catalyst, substituting methanol for higher alcohols resulted in lower yields of the corresponding pentenoate esters after 25 h of reaction (80 mol% for methanol, 20 mol% for ethanol and 2-3 mol% for butanol). In summary, this work showed that Brønsted acidity seems relevant to promote the GVL ring-opening when methanol is used as reactant and solvent. This is in agreement with our results previously commented, where acidic catalysts based on exclusively Lewis acidity were not successful for producing the PP intermediate from GVL and PL. In other words, when the acidity role on the GVL ring-opening with PL was studied over monofunctional acidic solids, both Lewis and Brønsted acidity seemed to be relevant for promoting the consecutive acid-catalyzed steps along ROUTE 2. Nevertheless, bifunctional catalysts based on Cu/SiO_2 containing very small Cu particles (prepared by chemisorption–hydrolysis method) that exhibited exclusively Lewis acidity also shown to be efficient for producing PV from GVL and PL [54]. This is suggesting that, for ROUTE 2 of production of VE, systematic studies where the acidic support is selected previously to deposit the metal lead to different conclusions to those obtained in studies where acidic and metal catalytic functions are tested together in the bifunctional solid [64]. In other words, researchers' opinions about the acid requirements for obtaining VE from GVL and alcohol along ROUTE 2 seem controversial.

On the other hand, the authors that studied the production of VE along ROUTE 1 agree with the observations that Brønsted acidity is crucial for promoting the GVL ring-opening by the C4-O1 bond scission, producing the pentenoic acid intermediate that leads to the formation of PA in the presence of a metal and H_2. In summary, the acidity of the catalysts influences the reaction differently, depending if the VE formation takes place along ROUTE 1 or 2.

3.3. A brief assessment of the one-pot processes for valeric biofuel production from GVL

Some relevant features and consequences of both ROUTES 1 and 2 deserve to be addressed when a general assessment of these technologies is carried out. Although operative conditions regarding thermal levels and H_2 pressures are quite similar for both routes, the use of an excess of alcohol when the valeric ester production is performed along ROUTE 2 makes a huge difference. ROUTE 1 does not require the use of an alcohol as solvent, though the use of a solvent is necessary in order to: (1) to dissolve reactants (GVL and H_2) and products allowing a better transport to/from the catalyst surface; (2) to control the reactant conversion rate in the case of very rapid chemical reactions; (3) to dissipate the heat generated in exothermic reactions. However, if the desired valeric ester is formed along ROUTE 1, the alcohol with the appropriate alkyl chain will be needed to react with PA over acidic sites. When PV is the target biofuel, no extra alcohol is needed because PL can be formed from PA by successive reduction, but in the case of EV, ethanol

must be fed to the reactor. In contrast, in the case of ROUTE 2, the use of the alcohol as solvent is absolutely necessary to achieve the GVL ring-opening and generate the key intermediate. However, the use of alcohol as solvent and reactant is a clear disadvantage not only from the economic point of view, but also from another point of view mostly ignored by other authors: byproduct formation from solvent. The presence of an acidic catalyst and a relatively high concentration of alcohol increase significantly the probability of side reactions, such as the intermolecular and intramolecular alcohol dehydration. The first one leads to the formation of the dialkyl ether, an undesirable reaction product that consumes the alcohol and could block catalytically active sites. The second undesirable reaction, the intramolecular alcohol dehydration, originates gaseous olefins that increase the pressure inside the reactor and can lead to the formation of carbonaceous residues over the acid sites, diminishing the catalytic performance.

For performing a general assessment of valeric biofuel production from GVL, particular attention must be put in the VE productivity attained, the reaction conditions (mainly H_2 pressure and reaction temperature) and characteristic of the catalyst (use of expensive noble metal, metal loadings and complexity of the preparation method). Table 2 compares the previously described reports about the production of valeric esters in one-pot processes and batch conditions.

In our opinion, though the first report of valeric esters production was in 2010, the conversion of GVL into valeric biofuels is still in an early stage. Only two years ago, some serious progress in the valeric ester productivity (300-660 $mmol.g_M^{-1}.h^{-1}$) was observed in batch conditions, mainly when noble metal-based catalysts (Pt, Rh and Pd) with moderate metal loadings ($\cong$1 wt%) were tested in ROUTE 2 for PV production [60][61]. Pd-based catalysts also showed interesting performances along ROUTE 1 but only when very high metal loading (5 wt%) and severe reaction conditions were employed [44]. In this case, the PV productivity was slightly lower than 90 mmol $g_M^{-1}.h^{-1}$, which can be considered an intermediate value among the reported values (Table 2). Besides, octane was used as inert solvent, but it is worth mentioning that: (i) octane is not a relatively cheap solvent; (ii) it is a highly volatile solvent that can lead to a dramatic increase of the pressure inside the reactor. On the other hand, along ROUTE 2, Cu-based samples have been the most studied catalysts that shown as advantages an appreciable activity and remarkable selectivity to PV with a relatively cheap metal but with a relatively complex catalyst preparation, except the work of Liu et al. {Formatting Citation}. For these works, EV productivity was between 25 and 96 mmol $g_M^{-1}.h^{-1}$ (Table 2). Ni-based catalysts supported on SiO_2-Al_2O_3 showed a lower catalytic performance in the PV production comparing with Cu-based samples, especially when precipitation-deposition is used for preparing the Ni catalysts [58]. In contrast, Co/HZSM-5 catalyst exhibits the highest EV productivity among the non-noble metal-based catalysts [55]. However, it is expected that the strong Brønsted acidity of this zeolite would promote side reaction such as intermolecular and/or intramolecular dehydration of the alcohol, leading to undesirable ethers and/or olefins coming from the alcohol solvent, as our group verified [62]. Regarding the use of noble metal-based catalysts, only our group prepared catalysts with a moderate metal loading ($\cong$1 wt%) to be tested in batch conditions, whereas Zhang et al. [59] attained a EV productivity of 166 $mmol.g_M^{-1}.h^{-1}$ over Pd/MIL-101-SO_3H(100) performing the reaction at 250 °C and 30 bar of H_2, but using a very expensive catalyst containing 5 wt% of Pd that

also deactivated (Table 2). In this sense, we have recently reported that SiO_2-Al_2O_3 seems to be an appropriate acid support for depositing a noble metal, with low-moderate loading ($\cong$1 wt%), in order to reach a PV productivity higher than 300 $mmol.g_M^{-1}.h^{-1}$ (Table 2).

Table 2. Reported values of productivity to valeric esters from GVL and reaction conditions employed in batch one-pot processes.

Best catalyst	Solvent	T (°C)	P_{H2} (bar)	$P_{VE}^{[b]}$ ($mmol.g_M^{-1}.h^{-1}$)	Ref.
Cu(8%)/SiO₂-ZrO₂	Ethanol	250	10	25.4	[36]
	Pentanol	250	10	47.7	
Cu(16%)/SiO₂	Pentanol	250	10	52.3	[54]
Cu(10%)/ZrO₂-ZnAl₂O₄	Methanol	240	10	98.9	[56]
	Ethanol	240	10	99.9	
	Propanol	250	10	94.9	
	Butanol	250	10	93.8	
	Pentanol	250	10	91.8	
Cu(10%)/ZrO₂	Methanol	230	15	95.2	[57]
	Ethanol	230	15	89.6	
	Propanol	230	15	72.6	
	Isopropanol	230	15	46.8	
	Butanol	230	15	71.0	
	Pentanol	230	15	87.5	
	Isoamyl alcohol	230	15	38.7	
	Hexanol	230	15	74.1	
	Cyclohexanol	230	15	31.3	
Co(10%)/HZSM-5	Ethanol	240	30	213.6	[55]
Ni(7%)/SiO₂-Al₂O₃	Pentanol	250	10	58.0	[58]
Pd(5%)/MIL-101-SO₃H	Ethanol	250	30	166.0	[59]
Pd(5%)/HY	Octane	260	80	88.8	[44]
Pt(1%)/SiO₂-Al₂O₃	Pentanol	250	10	300.1	[60]
Rh(1%)/SiO₂-Al₂O₃	Pentanol	250	10	376.5	[61]
Pd(1%)/SiO₂-Al₂O₃	Pentanol	250	10	660.7	

Last but not the least, when ROUTE 1 and 2 are compared, it is worth mentioning that ROUTE 2 offers more possibilities for process integration at industrial scale, because along ROUTE 1 once the key intermediate PA is produced, the alcohol needed to form the VE must be fed into the reaction system, employing an

assisted tandem methodology that makes the one-pot process more complex. Only in the case of PV production the alcohol is not required as reactant because PL can be formed from PA by reduction. In contrast, along ROUTE 2, the alcohol must be present from the outset, playing both roles, as solvent and reactant, not being necessary a further addition comprising an assisted tandem methodology.

4. Economic aspects of VE production

To make an economic analysis on the commercial prospects of valeric biofuels we must consider that, although the prices of VE are strongly conditioned by the prices of fossil fuels, the oil reserves will inexorably run out [65]. Therefore, VE as other second generation biofuels are likely to become a part of the solution for shifting the transportation sector of the energy demand towards more sustainable alternatives in the medium-term.

Thirteen years have passed since the catalytic production and use of valeric esters were firstly reported but no production plants have been built yet. Different reasons have delayed the investments in this field, such as the discovery of big reserves of shale oil and gas in different countries. This fact moved the public and scientific attention to these fossil reserves which, though are non-sustainable, are very compatible with the installed capacity and technology of the present refineries.

Only very few works providing economic information about second-generation biofuels (but not for VE) are found in the literature [29,65–67]. In this scenario, trying to perform an economic evaluation or assessment of the VE production seems a little bit difficult. Nevertheless, ten relevant points can be highlighted when the economic feasibility of the production and use of the valeric biofuels is evaluated:

1) Many researchers have pointed out that, though VE are second-generation biofuels because they are produced from non-edible biomass, these biofuels compete with food crops for arable land. However, in countries with vast territories, unsuitable or low-yielding land can be used for energy crops without affecting the food crop production. Thus, large countries, such as Argentina, exhibit great potential for the production of VE, not only from forest and agricultural wastes, but also from energy crops grown in less favorable lands [67].

2) An efficient organization of supply chain logistics is required, especially for the low energy density feedstocks that, probably, will need an early-densification in the chain. This is critical in the case of using agricultural wastes such as wheat and rice straw [68,69].

3) Production costs of VE from GVL are uncertain because the biomass origin can be very diverse and, therefore, the GVL yield obtained from the biomass is variable [70].

4) The market price of GVL is still too high to consider it as raw material for producing valeric esters, so isolated processes based exclusively on the conversion of GVL into valeric esters are, by far, not economically viable. However, the global biofuel market is expected to grow with a CAGR of 8% between 2019 and 2024 [71]. This envisions the installation of more biorefineries worldwide that will contribute to reduce the GVL market price.

5) There are some technical barriers that remain relatively high, such as the necessity of increasing the VE productivity values [16]. In this sense, different catalytic systems are being tested in batch processes before moving to continuous processes, where operative costs can be reduced for a larger production.

6) Production routes of valeric esters must be unfailingly linked to the concept of the integrated biorefinery. This concept involves the combination of several technologies (thermochemical, biochemical, etc.) to reduce the overall cost, produce a greater variety of valuable products and self-supply energy [29][72]. For instance, Zhang et al. conducted an economic feasibility analysis of the production of second-generation biofuels (in this case liquid fuels by Fischer-Tropsch) based on pyrolysis integrated with bio-oils gasification using corn stover as cellulose feedstock and determined that the deployment of the plant would require 2000 tons of biomass per day requiring a capital investment of 510 million dollars to make this integrated process economically and technically viable [73]. Although there are not works like this in the literature about valeric biofuels production, undoubtedly the concept of integrated biorefinery could bring a solution for the supply of the alcohol employed if ROUTE 2 is used for the VE synthesis.

7) Valeric esters, as other second-generation biofuels, will probably not become economically feasible for another decade, even with oil prices remain above USD 80/bbl. Only if oil prices remain consistently over USD 100/bbl, valeric esters will be commercially competitive with oil products as liquid fuels for transportation [66].

8) Both public and private sectors must play active roles, sharing risks for investing in research, development, demonstration and deployment of these technologies, especially in developing countries with a considerable agricultural potential [66].

9) Biofuels in general and VE in particular represent great potential in three key areas: national energy self-sufficiency, reduction of environmental pollution and job creation in rural areas. Government regulations become essential to help this industry emerge, such as regulations on fossil/biofuel blend specifications, financial incentives and import restrictions that protect domestic biofuel producers [74].

10) The potential of valeric esters as transportation fuels can be considered only in a long-term view, but the necessary investment to improve these technologies must not be delayed more time [66].

5. Concluding remarks and future perspective

Thirteen years have passed since Lange et al. reported the first production and use of valeric esters as second-generation biofuels in a continuous process. From that moment, in the majority of published works the authors have studied the γ-valerolactone conversion in batch mode using bifunctional catalytic systems that rely on orthogonal tandem catalysis. In these relatively complex catalytic systems, both acidic and metal functions work together in order to consecutively transform the intermediates into the valuable valeric esters. These liquid-phase processes follow either reaction ROUTE 1 or 2. If the solvent is not an alcohol, the acid-catalyzed ring-opening of GVL leads to pentenoic acid following ROUTE 1, not detectable in liquid phase. Then pentenoic acid is easily hydrogenated into pentanoic acid (PA). This key intermediate must be esterified with the appropriate alcohol to form the desired VE. On the other hand, if the one-pot process is carried out in the presence of alcohol, the acid-catalyzed ring opening of GVL takes place by the nucleophilic attack of the alcohol, forming a highly reactive intermediate (HPV) that is consecutively dehydrated into an alkyl pentenoate. This intramolecular dehydration seems to be the most difficult reaction regarding the acid-requirement of the catalyst. Finally, over the metal sites that chemisorb hydrogen

dissociatively, the hydrogenation of the alkyl pentenoate to the alkyl valerate takes place. Following this ROUTE 2 several alkyl valerates have been produced with different fuel properties depending on the alkyl chain.

Although the ROUTE 1 shows the evident advantage of avoiding the use of alcohol as solvent, apparently the reaction conditions must be more severe, and the metal loadings of noble metal-based catalysts employed so far are very high. Surprisingly, no more works exploring ROUTE 1 has been published since 2015, in contrast with ROUTE 2, where present work is mostly carried out. Nevertheless, for both reaction routes, the main efforts must be focused on improving the valeric ester productivity in batch conditions. In this sense, the ultimate works employing noble metal-based catalysts seem to go in the right way, though reducing the metal loading to values lower than 1% is highly desirable to decrease the cost of catalysts. Besides, particular attention to the deactivation of the catalysts in these conditions must be paid, performing specific studies about this relevant subject for achieving a future successful implementation of continuous catalytic processes.

In particular, if ROUTE 2 is selected using relatively cheap non-noble metal-based catalysts such as Cu, the main challenges are to simplify catalyst preparation and improve the catalyst activity avoiding metal leaching. Disregarding if noble or non-noble metal-based catalysts are used, a fine tuning of the metal dispersion and acid site density seems to be the key for preparing highly active, selective and stable acid/metal bifunctional catalysts to perform efficiently the required orthogonal tandem catalysis. In this sense, studying separately the acid requirements of the catalytic support and the metal hydrogenation capacity has shown clear advantages for designing an efficient catalytic system.

Undoubtedly, for a liquid-phase one-pot process is highly desirable to use milder reaction conditions than those reported. However, performing these orthogonal tandem catalytic reactions with appreciable activity at temperatures lower than 230-260 °C seems impossible up to now. However, not extremely high H_2 pressure values (e.g. 10 bar) have been reported, indicating that the availability of H_2 even at these pressures is enough to convert the unsaturated intermediates into the valuable esters, though the hydrogen chemisorption capacity of the metal influences the hydrogenation activity.

Although a quite efficient acidic support (SiO_2-Al_2O_3) has been identified and selected for preparing bifunctional catalysts, especially for ROUTE 2, some aspects remain unknown, such as if the production of undesirable pentyl 4-pentoxy valerate (PPV) can be reduced even more. In this sense, the GVL/alcohol ratio seems to be a promising experimental parameter to be modified. Besides, the formation of PPV depends strongly on the acid properties of the catalyst and future studies regarding the tuning of density/strength of acid sites seem necessary to diminish the selectivity towards this undesirable product and to increase the selectivity towards pentyl pentenoate (PP), the desired final product of the acid catalysis involved. Due to the complexity of both ROUTE 1 and ROUTE 2 and the necessity that acid sites work in cooperation with metal sites to achieve an efficient orthogonal tandem catalysis, more studies must be carried out in order to improve the VE productivity in these batch one-pot processes. Once higher VE productivity values are reached, the implementation of continuous catalytic processes for a massive valeric biofuel production can be thought.

REVIEW

WILEY-VCH

Last but not the least, the pursuit of boosting the valeric ester productivity should motivate the catalytic community to perform systematic studies where isolated experiments of the acid-catalyzed steps and the hydrogenation step are considered [64]. In this sense, this kind of studies make possible to select an appropriate acid support and an active metal function that, comprising a bifunctional acid/metal catalyst, attain a high GVL conversion and valerate ester yield in shorter times, leading to much higher values of valeric ester productivity. Only the best catalytic formulations in terms of valeric ester productivity and stability selected from batch studies will be considered as serious candidates for the bifunctional catalysts to be used in liquid-phase continuous processes for producing these biofuels. If this is eventually achieved, the production of gasoline- and diesel-type second-generation biofuels for supplying the transportation sector in a renewable way will become a palpable reality.

Acknowledgements

References

[1] S. Sorrell, J. Speirs, R. Bentley, A. Brandt, R. Miller, *An Assessment of the Evidence for a Near-Term Peak in Global Oil Production*, London, U.K., **2009**.

[2] K. Perry, J. Lee, *Work. Doc. NPC Glob. Oil Gas Study* **2007**, *18*.

[3] S. Lu, W. Huang, F. Chen, J. Li, M. Wang, H. Xue, W. Wang, X. Cai, *Pet. Explor. Dev.* **2012**, *39*, 268–276.

[4] B. A. Babb, M. K. Pruett, *Mon. Energy Rev.* **2019**, *57*, 155–157.

[5] S. Zinoviev, F. Müller-Langer, P. Das, N. Bertero, P. Fornasiero, M. Kaltschmitt, G. Centi, S. Miertus, *ChemSusChem* **2010**, *3*, 1106–1133.

[6] D. M. Alonso, J. Q. Bond, J. A. Dumesic, *Green Chem.* **2010**, *12*, 1493–1513.

[7] R. D. Perlack, L. L. Wright, A. F. Turhollow, R. L. Graham, B. J. Stokes, D. C. Erbach, *Biomass as Feedstock for a Bioenergy and Bioproducts Industry : The Technical Feasibility of a Billion-Ton Annual Supply*, US Department Of Energy And US Department Of Agriculture, **2005**.

[8] G. W. Huber, B. E. Dale, *Sci. Am.* **2009**, *301*, 52–59.

[9] F. H. Isikgor, C. R. Becer, *Polym. Chem.* **2015**, *6*, 4497–4559.

[10] P. Gallezot, *Chem. Soc. Rev.* **2012**, *41*, 1538–1558.

[11] J. J. Bozell, *Science (80-.).* **2010**, *329*, 522–523.

[12] J. J. Bozell, G. R. Petersen, *Green Chem.* **2010**, *12*, 539–55.

[13] I. T. Horváth, H. Mehdi, V. Fábos, L. Boda, L. T. Mika, *Green Chem.* **2008**, *10*, 238–24.

[14] F. Kerkel, M. Markiewicz, S. Stolte, E. Müller, W. Kunz, *Green Chem.* **2021**, *23*, 2962–2976.

[15] D. M. Alonso, S. G. Wettstein, J. A. Dumesic, *Green Chem.* **2013**, *15*, 584–595.

[16] K. Yan, Y. Yang, J. Chai, Y. Lu, *Appl. Catal. B Environ.* **2015**, *179*, 292–304.

[17] H. Li, Z. Fang, S. Yang, *Chempluschem* **2016**, *81*, 135–142.

[18] H. Xu, D. Hu, L. Lin, M. Zhang, K. Yan, M. Amer, *AIChE J.* **2023**, *69*, 17973–17982.

[19] W. R. H. Wright, R. Palkovits, *ChemSusChem* **2012**, *5*, 1657–1667.

[20] H. Li, Z. Fang, R. L. Smith, S. Yang, *Prog. Energy Combust. Sci.* **2016**, *55*, 98–194.

[21] M. Besson, P. Gallezot, C. Pinel, *Chem. Rev.* **2014**, *114*, 1827–1870.

[22] M. J. Climent, A. Corma, S. Iborra, *Green Chem.* **2014**, *16*, 516–547.

[23] K. Yan, C. Jarvis, J. Gu, Y. Yan, *Renew. Sustain. Energy Rev.* **2015**, *51*, 986–997.

[24] J. P. Lange, R. Price, P. M. Ayoub, J. Louis, L. Petrus, L. Clarke, H. Gosselink, *Angew. Chemie - Int. Ed.* **2010**, *49*, 4479–4483.

[25] F. Oppong, C. Xu, X. Li, Z. Luo, *Fuel Process. Technol.* **2022**, *229*, 107185.

[26] F. Contino, P. Dagaut, G. Dayma, F. Halter, F. Foucher, C. Mounaïm-Rousselle, *J. Energy Eng.* **2014**, *140*, 1–7.

[27] M. Boot, in *Biofuels from Lignocellul. Biomass Innov. beyond Bioethanol* (Ed.: M. Boot), Wiley-VCH Verlag GmbH & Co., Weinheim, Germany, **2015**, pp. 1–214.

[28] F. Contino, F. Foucher, F. Halter, G. Dayma, P. Dagaut, C. Mounaïm-Rousselle, *SAE Tech. Pap.* **2013**, *24*, 98–103.

[29] S. N. Naik, V. V Goud, P. K. Rout, A. K. Dalai, **2010**, *14*, 578–597.

[30] P. Cazzola, G. Morrison, H. Kaneko, F. Cuenot, A. Ghandi, L. Fulton, *Production Costs of Alternative Transportation Fuels*, **2013**.

[31] S. N. Derle, P. A. Parikh, *Biomass Convers. Biorefinery* **2014**, *4*, 293–299.

[32] M. Sajid, U. Farooq, G. Bary, M. Mohsin Azim, X. Zhao, *Green Chem.* **2021**, *23*, 9198–9238.

[33] R. J. Haan, J.-P. Lange, *Process for Preparing an Ester*, **2010**, US 9.012,680 B2.

[34] Z. Yu, X. Lu, J. Xiong, N. Ji, *ChemSusChem* **2019**, *12*, 3915–3930.

[35] R. Pothu, R. Gundeboyina, R. Boddula, V. Perugopu, J. Ma, *New J. Chem.* **2022**, *46*, 5907–5921.

[36] C. E. Chan-Thaw, M. Marelli, R. Psaro, N. Ravasio, F. Zaccheria, *RSC Adv.* **2013**, *3*, 1302–1306.

[37] H. Wang, Q. Wang, Y. Wu, J. Peng, X. Gu, M. Ding, *Chem. Eng. J.* **2022**, *446*, 137404.

[38] H. Wang, Q. Wang, Y. Tong, Y. Wu, J. Peng, X. Gu, M. Ding, *Appl. Catal. B Environ.* **2022**, *318*, 121840.

[39] H. Wang, Q. Wang, Y. Wu, J. Peng, X. Gu, M. Ding, *ACS Catal.* **2022**, *12*, 12027–12035.

[40] H. Wang, Y. Wu, Y. Li, J. Peng, X. Gu, M. Ding, *Appl. Catal. B Environ.* **2021**, *296*, 120338.

[41] H. Wang, Y. Wu, Y. Li, J. Peng, X.-K. Gu, M. Ding, *Green Chem.* **2021**, *23*, 4780–4789.

[42] A. Rozenblit, A. J. Avoian, Q. Tan, T. Sooknoi, D. E. Resasco, *J. Energy Chem.* **2016**, *25*, 1008–1014.

[43] R. M. Bababrik, B. Wang, D. E. Resasco, *Ind. Eng. Chem. Res.* **2017**, *56*, 3217–3222.

[44] K. Yan, T. Lafleur, X. Wu, J. Chai, G. Wu, X. Xie, *Chem. Commun.* **2015**, *51*, 6984–6987.

[45] D. E. Fogg, E. N. Dos Santos, *Coord. Chem. Rev.* **2004**, *248*, 2365–2379.

[46] G. Novodárszki, H. E. Solt, G. Lendvay, R. M. Mihályi, A. Vikár, F. Lónyi, J. Hancsók, J. Valyon, *Catal. Today* **2019**, *336*, 50–62.

[47] K. Kon, W. Onodera, K. I. Shimizu, *Catal. Sci. Technol.* **2014**, *4*,

3227–3234.

[48] Q. Xu, X. Li, T. Pan, C. Yu, J. Deng, Q. Guo, Y. Fu, *Green Chem.* **2016**, *18*, 1287–1294.

[49] J. C. Serrano-ruiz, D. Wang, J. a Dumesic, *Green Chem.* **2010**, *3*, 2–3.

[50] J. C. Serrano-Ruiz, D. J. Braden, R. M. West, J. A. Dumesic, *Appl. Catal. B Environ.* **2010**, *100*, 184–189.

[51] J. C. Serrano-Ruiz, D. Wang, J. A. Dumesic, *Green Chem.* **2010**, *12*, 574–577.

[52] H. Wang, Y. Wu, Y. Li, J. Peng, X. K. Gu, M. Ding, *Appl. Catal. B Environ.* **2021**, *296*, 120338.

[53] D. Velisoju, Vijay Kumar Jampaiah, N. Gutta, U. Bentrup, A. Brückner, S. K. Bhargava, V. Akula, *ChemCatChem* **2020**, DOI 10.1002/cctc.201901966.

[54] N. Scotti, M. Dangate, A. Gervasini, C. Evangelisti, N. Ravasio, F. Zaccheria, *ACS Catal.* **2014**, *4*, 2818–2826.

[55] P. Sun, G. Gao, Z. Zhao, C. Xia, F. Li, *ACS Catal.* **2014**, *4*, 4136–4142.

[56] W. Li, Y. Li, G. Fan, L. Yang, F. Li, *ACS Sustain. Chem. Eng.* **2017**, *5*, 2282–2291.

[57] S. Liu, G. Fan, L. Yang, F. Li, *Appl. Catal. A Gen.* **2017**, *543*, 180–188.

[58] K. G. Martínez Figueredo, D. J. Segobia, N. M. Bertero, *Catal. Commun.* **2020**, *144*, 106087.

[59] D. Zhang, F. Ye, Y. Guan, Y. Wang, E. J. M. Hensen, *RSC Adv.* **2014**, *4*, 39558–39564.

[60] K. G. Martínez Figueredo, E. M. Virgilio, D. J. Segobia, N. M. Bertero, *Chempluschem* **2021**, *86*, 1342–1346.

[61] K. G. Martínez Figueredo, E. M. Virgilio, D. J. Segobia, N. M. Bertero, *React. Chem. Eng.* **2022**, DOI 10.1039/D2RE00121G.

[62] K. G. Martínez Figueredo, D. J. Segobia, N. M. Bertero, *Energy Convers. Manag. X* **2022**, *13*, 100162.

[63] J. P. Lange, J. Z. Vestering, R. J. Haan, *Chem. Commun.* **2007**, 3488–3490.

[64] K. G. Martínez Figueredo, D. J. Segobia, N. M. Bertero, in *Adv. Chem. Res. Vol. 81* (Ed.: J.C. Taylor), Nova Science Publishers, Inc., **2023**, p. Chapter 3.

[65] M. Kashif, A. Batool, A. Kashif, M. Haq, M. Aslam, N. Iqbal, Y. Choi, *J. Environ. Manage.* **2021**, *297*, 113268.

[66] R. E. H. Sims, W. Mabee, J. N. Saddler, M. Taylor, *Bioresour. Technol.* **2010**, *101*, 1570–1580.

[67] S. G. Mungodla, L. Z. Linganiso, S. Mlambo, T. Motaung, S. G. Mungodla, L. Z. Linganiso, S. Mlambo, T. Motaung, S. G. Mungodla, *J. Eng. Des. Technol.* **2019**, *17*, 670–704.

[68] K. K. Castillo-Villar, S. Eksioglu, M. Taherkhorsandi, *J. Clean. Prod.* **2017**, *149*, 904–918.

[69] W. Liu, C. Lin, T. Yeh, *Energy* **2017**, *139*, 630–645.

[70] L. Ye, Y. Han, J. Feng, X. Lu, *Ind. Crop. Prod.* **2020**, *144*, 112031.

[71] M. Clauser, F. E. Felissia, M. C. Area, M. E. Vallejos, *Renew. Sustain. Energy Rev.* **2021**, *139*, 110687.

[72] T. Damartzis, A. Zabaniotou, *Renew. Sustain. Energy Rev.* **2011**, *15*, 366–378.

[73] Y. Zhang, T. R. Brown, G. Hu, R. C. Brown, *Biomass and Bioenergy* **2013**, *51*, 99–108.

[74] V. Fantin, A. Giuliano, M. Manfredi, G. Ottaviano, M. Stefanova, P. Masoni, *Biomass and Bioenergy* **2015**, *83*, 422–435.

Karla Martínez Figueredo completed her PhD career in Chemistry at FIQ-UNL (Universidad Nacional del Litoral) in 2022 under the supervision of Prof. Nicolás Bertero in the Catalysis Science and Engineering Research Group (GICIC). Previously, she obtained her Bachelor's Degree in Chemistry at Universidad Central de Venezuela in 2015. Currently, she is working at Universidad Católica de Santa Fe as Assistant Professor and performing postdoctoral studies on metallocorroles as electrocatalysts in synthetic organic reactions at INTEC-CONICET. Her research interests are focused on materials and their potential use in the production of valuable chemicals by tandem catalysis and electrocatalysis.

Francisco Martínez obtained his Bachelor's Degree in Engineering at Universidad Nacional de Villa Mercedes in 2023 in Argentina. Currently, during his PhD studies (Universidad Nacional del Litoral) carried out at the GICIC group of INCAPE, he is working under the supervision of Prof. Nicolás Bertero on the catalytic production of valeric biofuels from biomass-derived platform molecules over bifunctional solids.

Darío Segobia received his PhD degree in Chemical Engineering in 2013 from Universidad Nacional del Litoral, Santa Fe, Argentina. His PhD thesis, about the hydrogenation of nitriles to amines, was supervised by Dr. Carlos Apesteguía. After finishing his postdoctoral studies at the Institute of Research on Catalysis and Petrochemistry (INCAPE), Santa Fe, Argentina, he became a member of the CONICET's Research Staff. At the moment, he teaches at Universidad Nacional del Litoral and works in GICIC-INCAPE studying not only the production of valuable amines and imines on monofunctional catalysts, but also the catalytic conversion of γ-valerolactone into biofuels.

Nicolás Bertero obtained his PhD in Chemical Engineering in 2007 at Universidad Nacional del Litoral, Santa Fe, Argentina. After his postdoctoral fellowship in the Area of Chemistry at the ICS-UNIDO and University of Trieste under the supervision of Prof. Fornasiero (Italy, 2009), he joined the CONICET (Argentina) as a Researcher in 2010. His work at GICIC-INCAPE is mainly focused on the use of heterogeneous catalysis in fine chemical synthesis, environmental applications and biofuels. Particularly, he studies the production of second-generation biofuels and fine chemicals in liquid-phase processes employing tandem catalysis over monofunctional and multifunctional solid materials.
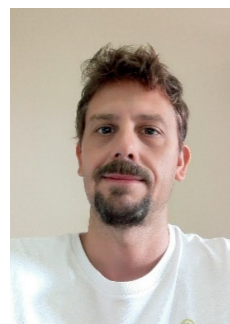
Entry for the Table of Contents
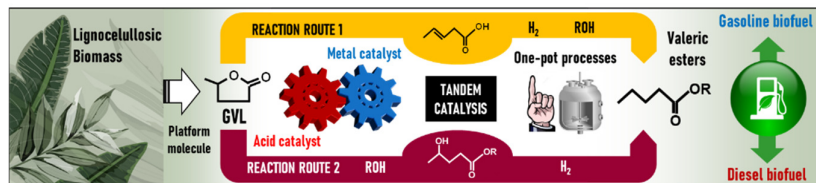
This work analyzes critically the reported technologies for the production of valeric biofuels from γ-valerolactone (GVL), a biomass-derived platform molecule. The review is focused on the effect of bifunctional catalysts and reaction conditions on the two possible reaction routes. Particular attention is devoted to the values of valeric ester productivity, which have been improved markedly in the last few years.